

This is a PDF file of the unedited manuscript that was accepted for publication:

**Nitrate and nitrite reduction by ferrous iron minerals in polluted groundwater: Isotopic characterization of batch experiments.**

Rosanna Margalef-Marti, Raúl Carrey, José Antonio Benito, Vicenç Marti, Albert Soler, Neus Otero

Chemical Geology, 2020

DOI: <https://doi.org/10.1016/j.chemgeo.2020.119691>

Received date: 23 January 2020

Revised date: 20 May 2020

Accepted date: 21 May 2020

Available online: 25 May 2020

1 **Nitrate and nitrite reduction by ferrous iron minerals in polluted**  
2 **groundwater: Isotopic characterization of batch experiments**

3  
4 Rosanna Margalef-Martí<sup>1,2</sup>, Raúl Carrey<sup>1,2</sup>, José Antonio Benito<sup>3</sup>, Vicenç Martí<sup>3</sup>, Albert  
5 Soler<sup>1,2</sup>, Neus Otero<sup>1,2,4</sup>

6  
7 <sup>1</sup> Grup MAiMA, SGR Mineralogia Aplicada, Geoquímica i Geomicrobiologia, SIMGEO  
8 UB-CSIC, Departament de Mineralogia, Petrologia i Geologia Aplicada, Facultat de  
9 Ciències de la Terra, Universitat de Barcelona (UB), C/Martí i Franquès s/n,  
10 08028 Barcelona (Spain).

11 <sup>2</sup> Institut de Recerca de l'Aigua (IdRA), UB, 08001 Barcelona (Spain).

12 <sup>3</sup> Materials Science and Metallurgical Engineering Department and Barcelona  
13 Research Center in Multiscale Science and Engineering, EEBE, Technical University of  
14 Catalonia (UPC), Av. Eduard Maristany 16, 08019 Barcelona (Spain).

15 <sup>4</sup> Serra Húnter Fellowship, Generalitat de Catalunya (Spain).

16  
17 **ABSTRACT**

18 Since nitrate ( $\text{NO}_3^-$ ) has been related to human health and environmental problems,  
19 safe and sustainable strategies to remediate polluted water bodies must be  
20 investigated. This work aims to assess the feasibility of using ferrous iron (Fe(II))-  
21 containing minerals to stimulate microbial denitrification while avoiding pollution  
22 swapping (e.g. accumulation of the by-products nitrite ( $\text{NO}_2^-$ ) or nitrous oxide ( $\text{N}_2\text{O}$ )).  
23 To accomplish the objective, samples obtained from several batch experiments were

1  
2  
3  
4  
5  
6  
7  
8  
9  
10  
11  
12  
13  
14  
15  
16  
17  
18  
19  
20  
21  
22  
23  
24  
25  
26  
27  
28  
29  
30  
31  
32  
33  
34  
35  
36  
37  
38  
39  
40  
41  
42  
43  
44  
45  
46  
47  
48  
49  
50  
51  
52  
53  
54  
55  
56  
57  
58  
59  
60  
61  
62  
63  
64  
65

24 characterized chemically and isotopically. Magnetite, siderite and olivine were tested  
25 micro-sized and magnetite was also tested nano-sized. In microbial experiments,  $\text{NO}_3^-$   
26 polluted groundwater was employed as inoculum. In these experiments,  $\text{NO}_3^-$  reduction  
27 to nitrogen gas ( $\text{N}_2$ ) was only completed in microcosms containing magnetite  
28 nanoparticles, suggesting an increased Fe(II) availability from nano-sized compared to  
29 micro-sized magnetite. In abiotic experiments, no reactivity was observed between  
30  $\text{NO}_3^-$  or  $\text{NO}_2^-$  and micro-sized magnetite, siderite or olivine, while  $\text{NO}_2^-$  was rapidly  
31 reduced when dissolved  $\text{Fe}^{2+}$  was added. These results point to the need of a certain  
32 amount of dissolved  $\text{Fe}^{2+}$  to stimulate the abiotic  $\text{NO}_2^-$  reduction by Fe(II) oxidation. For  
33 the microbial  $\text{NO}_3^-$  reduction by magnetite nanoparticles, the calculated  $\epsilon^{15}\text{N}_{\text{NO}_3}$  was -  
34 33.1 ‰ ( $R^2 = 0.86$ ),  $\epsilon^{18}\text{O}_{\text{NO}_3}$  was -10.7 ‰ ( $R^2 = 0.74$ ) and  $\epsilon^{15}\text{N}_{\text{NO}_3}/\epsilon^{18}\text{O}_{\text{NO}_3}$  was 3.1. For  
35 the abiotic  $\text{NO}_2^-$  reduction by  $\text{Fe}^{2+}$ , the  $\epsilon^{15}\text{N}_{\text{NO}_2}$  ranged from -14.1 to -17.8 ‰ ( $R^2 >$   
36 0.89). Considering the wide range of  $\epsilon^{15}\text{N}_{\text{NO}_2}$  reported in the literature, it is not likely that  
37  $\text{NO}_2^-$  isotopic characterization can be useful at field-scale to distinguish abiotic from  
38 microbial  $\text{NO}_2^-$  reduction. Nevertheless, the measured  $\delta^{15}\text{N}$  for  $\text{N}_2\text{O}$  in microbial and  
39 abiotic tests, allowed to determine if it was an intermediate or a final product of the  
40 reactions by comparing these results with the modelled isotopic composition calculated  
41 using the  $\epsilon^{15}\text{N}$  values determined for the substrates. Hence, isotopic data confirmed  
42 that the product of the microbial  $\text{NO}_3^-$  reduction was innocuous  $\text{N}_2$  while the product of  
43 the abiotic  $\text{NO}_2^-$  reduction was  $\text{N}_2\text{O}$ . The latter reaction would be advantageous to  
44 avoid  $\text{NO}_2^-$  accumulation during denitrification only if the generated  $\text{N}_2\text{O}$  is further  
45 reduced by microorganisms.

46  
47 **Keywords:** abiotic nitrite reduction, denitrification, isotopic fractionation, magnetite  
48 nanoparticles, nitrous oxide

## 50 1. INTRODUCTION

1  
2  
3 51 Nitrate ( $\text{NO}_3^-$ ) has been related to human health disorders such as cancer and blue  
4  
5 52 baby syndrome and to environmental problems such as eutrophication of water bodies  
6  
7 53 (Rivett et al., 2008; Vitousek et al., 1997; Ward et al., 2005). Due to decades of  
8  
9 54 excessive crop fertilization and septic system leakage,  $\text{NO}_3^-$  is widely found in  
10  
11 55 groundwater. Consequently, since 1991, European directives (2006/118/EC, 2006;  
12  
13 56 91/676/EEC, 1991; 98/83/EC, 1998) have arisen to face the  $\text{NO}_3^-$  pollution persistence.  
14  
15  
16 57 One of the measures that can be implemented to attenuate the  $\text{NO}_3^-$  concentration in  
17  
18 58 water bodies is the addition of external electron donors to promote the denitrification,  
19  
20 59 since these compounds are usually deficient at field-scale (Rivett et al., 2008). The  
21  
22 60  $\text{NO}_3^-$  is reduced to innocuous nitrogen gas ( $\text{N}_2$ ) simultaneously to the oxidation of an  
23  
24 61 electron donor by denitrifying microorganisms (Borden et al., 2012; Böttcher et al.,  
25  
26 62 1990; Otero et al., 2009; Smith et al., 2001). However, intermediate N compounds can  
27  
28 63 be generated and accumulated since denitrification occurs through a series of  
29  
30 64 enzymatic reactions involving the conversion of  $\text{NO}_3^-$  to nitrite ( $\text{NO}_2^-$ ), nitric oxide (NO),  
31  
32 65 nitrous oxide ( $\text{N}_2\text{O}$ ) and finally  $\text{N}_2$  (Betlach and Tiedje, 1981; Knowles, 1982; Vidal-  
33  
34 66 Gavilan et al., 2013; Weymann et al., 2010). Not only  $\text{NO}_3^-$  but also these intermediate  
35  
36 67 N compounds have been recognized to produce detrimental effects for the environment  
37  
38 68 and human health (Badr and Probert, 1993; Vitousek et al., 1997; Ward et al., 2005).  
39  
40 69 Therefore, pollution swapping should be avoided when stimulating denitrification at  
41  
42 70 field-scale.  
43  
44  
45  
46  
47

48 71 In the search of economical and sustainable electron donors at laboratory-scale,  
49  
50 72 diverse industrial and agricultural waste products rich in organic carbon (C) have  
51  
52 73 proved to stimulate heterotrophic denitrification (Carrey et al., 2018; Gibert et al., 2008;  
53  
54 74 Margalef-Marti et al., 2019b; Si et al., 2018; Trois et al., 2010), while ferrous iron  
55  
56 75 ( $\text{Fe(II)}$ )-containing minerals such as pyrite, pyrrothite or biotite showed to stimulate  
57  
58 76 lithoautotrophic denitrification (Aquilina et al., 2018; Bosch et al., 2012; Torrentó et al.,  
59  
60  
61  
62  
63  
64  
65

1  
2  
3  
4  
5  
6  
7  
8  
9  
10  
11  
12  
13  
14  
15  
16  
17  
18  
19  
20  
21  
22  
23  
24  
25  
26  
27  
28  
29  
30  
31  
32  
33  
34  
35  
36  
37  
38  
39  
40  
41  
42  
43  
44  
45  
46  
47  
48  
49  
50  
51  
52  
53  
54  
55  
56  
57  
58  
59  
60  
61  
62  
63  
64  
65

77 2011; Yan et al., 2019; Yang et al., 2017). In the case of pyrite, it has been recently  
78 suggested that  $\text{NO}_3^-$  reduction might be stimulated by S instead of Fe oxidation (Yan et  
79 al., 2019). Also, a potential  $\text{NO}_3^-$  reactivity with the Fe(II,III) minerals green rust and  
80 magnetite has been observed (Byrne et al., 2015; Dhakal et al., 2013; Pantke et al.,  
81 2012). On the other hand, since mineral nanoparticles (NP) (e.g.  
82 Fe(III)(oxyhydr)oxides) are usually more reactive than macroparticles, their potential  
83 use to remediate polluted water bodies has gained attraction during the last years  
84 (Braunschweig et al., 2013). Materials such as Fe(0)-NP, magnetite-NP, Fe(III)oxide-  
85 NP or magnetite/maghemite-NP have been found to remove different organic and  
86 inorganic contaminants (Chowdhury and Yanful, 2010; Crane et al., 2011; Zelmanov  
87 and Semiat, 2008). Regarding  $\text{NO}_3^-$ , pyrite-NP, zeolite supported Fe/Ni-NP and  
88 Fe(0)/magnetite-NP could attenuate the pollution (Bosch et al., 2012; Cho et al., 2015b,  
89 2015a; He et al., 2018).

90 In the aforementioned microbial denitrification studies, a transient  $\text{NO}_2^-$  accumulation  
91 was generally observed (Ge et al., 2012; Torrentó et al., 2011; Yang et al., 2017), and  
92 although the gas emissions were not measured,  $\text{N}_2\text{O}$  accumulation cannot be  
93 discarded since this greenhouse gas (GHG) is usually detected during  $\text{NO}_3^-$  reduction  
94 both at laboratory and field-scale (Jurado et al., 2017; Margalef-Marti et al., 2019a;  
95 Morley et al., 2008; Weymann et al., 2010). During the last years, numerous studies  
96 have pointed that abiotic reactions involving the N and Fe biogeochemical cycles occur  
97 simultaneously to microbial denitrification (Carlson et al., 2013; Klueglein and Kappler,  
98 2013; Matocha and Coyne, 2007; Melton et al., 2014). The abiotic reduction of  $\text{NO}_2^-$  by  
99 Fe(II) oxidation have been well documented (Buchwald et al., 2016; Dhakal et al.,  
100 2013; Grabb et al., 2017; Rakshit et al., 2016), and might be advantageous to avoid a  
101 water quality decrease due to  $\text{NO}_2^-$  accumulation. However,  $\text{N}_2\text{O}$  has been proposed  
102 as the final product of this reaction (Buchwald et al., 2016; Chen et al., 2018; Coby and  
103 Picardal, 2005; Wang et al., 2016). Hence, supplying  $\text{NO}_3^-$  polluted water bodies with

1  
2  
3  
4  
5  
6  
7  
8  
9  
10  
11  
12  
13  
14  
15  
16  
17  
18  
19  
20  
21  
22  
23  
24  
25  
26  
27  
28  
29  
30  
31  
32  
33  
34  
35  
36  
37  
38  
39  
40  
41  
42  
43  
44  
45  
46  
47  
48  
49  
50  
51  
52  
53  
54  
55  
56  
57  
58  
59  
60  
61  
62  
63  
64  
65

104 Fe(II)-containing minerals to stimulate lithoautotrophic denitrification might promote  
105 N<sub>2</sub>O generation from both the microbial and abiotic NO<sub>2</sub><sup>-</sup> reduction. In laboratory  
106 experiments, Cooper et al. (2003) already found a larger N<sub>2</sub>O production during  
107 denitrification in the presence of Fe(II) compared to absence. Nevertheless, the  
108 accumulated N<sub>2</sub>O by both microbial and abiotic pathways could be further reduced by  
109 microorganisms in the presence of electron donors. The relative contribution of these  
110 two pathways of N<sub>2</sub>O production should be carefully assessed since the GHG is  
111 currently a focus of attention in climate change research (Reay et al., 2012).

112 The analysis of stable isotopes coupled to hydrochemical investigations is a widely  
113 accepted approach to understand biogeochemical processes in water bodies. The  
114 enzymatic NO<sub>3</sub><sup>-</sup> reduction provokes an enrichment in the heavy isotopes <sup>15</sup>N and <sup>18</sup>O of  
115 the unreacted substrate, unlike processes such as dilution that leads to a concentration  
116 decrease without influencing the isotopic signature (Böttcher et al., 1990; Fukada et al.,  
117 2003; Mariotti et al., 1981; Aravena and Robertson, 1998). The same pattern is  
118 expected throughout the enzymatic reduction of all N intermediate products (e.g. NO<sub>2</sub><sup>-</sup>  
119 or N<sub>2</sub>O), which will be initially depleted in <sup>15</sup>N and <sup>18</sup>O with respect to the substrate until  
120 the ultimate product will reach the NO<sub>3</sub><sup>-</sup> initial isotopic composition. Although the NO<sub>3</sub><sup>-</sup>  
121 isotopic evolution through heterotrophic denitrification has been widely studied (Carrey  
122 et al., 2014; Granger et al., 2008; Grau-Martínez et al., 2017; Wunderlich et al., 2012),  
123 the characterization during lithoautotrophic denitrification is scarce (Torrentó et al.,  
124 2011, 2010). Furthermore, information on the dual isotope systematics of NO<sub>2</sub><sup>-</sup> and  
125 N<sub>2</sub>O throughout its abiotic reduction by Fe(II) is still limited (Buchwald et al., 2016;  
126 Chen et al., 2018; Grabb et al., 2017; Jones et al., 2015). Therefore, it is not clear to  
127 which extent the isotopic characterization of NO<sub>3</sub><sup>-</sup>, NO<sub>2</sub><sup>-</sup> and N<sub>2</sub>O might help in  
128 distinguishing microbial and abiotic reactions involving the N and Fe biogeochemical  
129 cycles.

1  
2  
3  
4  
5  
6  
7  
8  
9  
10  
11  
12  
13  
14  
15  
16  
17  
18  
19  
20  
21  
22  
23  
24  
25  
26  
27  
28  
29  
30  
31  
32  
33  
34  
35  
36  
37  
38  
39  
40  
41  
42  
43  
44  
45  
46  
47  
48  
49  
50  
51  
52  
53  
54  
55  
56  
57  
58  
59  
60  
61  
62  
63  
64  
65

130 In this context, the aim of this work was to assess at laboratory-scale the suitability of  
131 using different Fe(II)-containing minerals to stimulate NO<sub>3</sub><sup>-</sup> reduction in groundwater  
132 (e.g. in permeable reactive barriers or by injection), while avoiding pollution swapping.  
133 The selected minerals were magnetite (Mag), siderite (Sd) and olivine (Ol), which were  
134 tested micro-sized. Mag was also tested nano-sized, to check changes in reactivity.  
135 Special attention was directed on the generation, accumulation and further reduction of  
136 the by-products NO<sub>2</sub><sup>-</sup> and N<sub>2</sub>O throughout the microbial NO<sub>3</sub><sup>-</sup> reduction. For this reason,  
137 the potential abiotic reactivity between NO<sub>3</sub><sup>-</sup> or NO<sub>2</sub><sup>-</sup> and Fe(II)-containing minerals or  
138 dissolved Fe<sup>2+</sup> was also evaluated. To accomplish the objective, the samples obtained  
139 from several batch experiments were characterized chemically and isotopically.

140

## 141 **2. METHODS**

### 142 *2.1. Batch experiments*

143 Micro-sized Mag, Ol and Sd and Mag-NP were tested to assess its potential use to  
144 stimulate microbial NO<sub>3</sub><sup>-</sup> reduction in laboratory batch experiments simulating aquifer  
145 conditions. Groundwater was obtained from well SMC-002 located in Roda de Ter  
146 (Barcelona, Spain). In this area, lithoautotrophic denitrification occurrence has been  
147 reported previously (Hernández-del Amo et al., 2018; Otero et al., 2009; Vitòria et al.,  
148 2008). In groundwater collected from the SMC-002 well, genes encoding the NO<sub>2</sub><sup>-</sup> and  
149 N<sub>2</sub>O reductases (nirS, nirK, and nosZ1) have also been detected and certain genus of  
150 denitrifying and Fe(II) oxidizing bacteria have been identified (Hernández-del Amo et  
151 al., 2018). Furthermore, aquifer geological material (mudstone) obtained from a similar  
152 nearby aquifer system was milled and then added in these microcosms to increase  
153 microbial diversity (hereafter named sediment). Hence, the series of experiments  
154 BioSedGW contained sediment, groundwater (1 mM NO<sub>3</sub><sup>-</sup>) and one of the selected  
155 minerals. Instead, the series BioSedDIW contained sediment, deionized water with

156  $\text{NaNO}_3$  (1 mM) and one of the selected minerals, which was employed as a control, to  
157 check a possible contribution of the sediment on the stimulated denitrification in the  
158 BioSedGW experiments. For the BioSedDIW experiments, it was assumed that  
159 denitrifying microorganisms were negligible in the deionized water and that the different  
160 chemical composition between deionized water and groundwater would not impart a  
161 significant effect on the sediment compounds dissolution. Both the BioSedGW and  
162 BioSedDIW series included a control without mineral. In addition, three bottles  
163 containing sediment and MilliQ water were incubated to determine a possible leakage  
164 of organic C from the sediment (blank experiments).

165 Micro-sized Mag, Ol and Sd were also tested to assess its potential abiotic reactivity  
166 with  $\text{NO}_3^-$  and  $\text{NO}_2^-$ . Three series of parallel anoxic incubations were performed. The  
167 series AbFeNO<sub>3</sub> contained  $\text{NO}_3^-$  rich synthetic water (1 mM), one of the three selected  
168 minerals and dissolved  $\text{Fe}^{2+}$ . The series AbFeNO<sub>2</sub> contained  $\text{NO}_2^-$  rich synthetic water  
169 (1 mM), one of the three selected minerals and dissolved  $\text{Fe}^{2+}$ . In both series dissolved  
170  $\text{Fe}^{2+}$  was added to maximize Fe(II) availability from a filtered  $\text{FeCl}_2 \cdot 4\text{H}_2\text{O}$  aqueous  
171 solution (5 mM). Finally, the series AbNO<sub>2</sub> contained  $\text{NO}_2^-$  rich synthetic water (1 mM)  
172 and one of the three selected minerals.

173 The detailed composition of each series of experiments is shown in **Table 1**. The main  
174 experiments (BioSedGw) involved 8 bottles for each mineral tested, two additional  
175 bottles were included in the case of Mag-NP. In contrast, the control experiments  
176 involved just 3 bottles, except for the AbFeNO<sub>2</sub> series that also involved 8 bottles to  
177 allow characterizing the abiotic  $\text{NO}_2^-$  reduction. The five series of batch experiments  
178 were set up inside a glove box, using 20 mL serum bottles, crimp sealed with butyl  
179 rubber stoppers under an Ar atmosphere. Incubations were performed at 23 °C and  
180 constant shaking in the darkness to avoid photodegradation processes. The bottles  
181 were sacrificed by turns at time intervals depending on the  $\text{NO}_3^-$  and  $\text{NO}_2^-$  reduction  
182 dynamics.



183 The characterization of the different types of water employed in the study is shown in  
184 the Supporting Information **Table S1**. The micro-sized minerals (Mag, Sd and Ol)  
185 preparation and Mag size reduction is explained in the Supporting Information **Section**  
186 **S1**. The mineral characterization is detailed in the Supporting Information **Section S2**.

## 187 *2.2. Analytical techniques*

188 All samples from the sacrificed bottles were filtered through 0.2  $\mu\text{m}$  Millipore® filter  
189 immediately when obtained and stored at 4 °C until analysis except aliquots for  
190 ammonium ( $\text{NH}_4^+$ ) concentration and isotopic characterization of N and O from  
191 dissolved  $\text{NO}_3^-$  and  $\text{NO}_2^-$  that were preserved frozen at -20 °C. Samples from  
192 experiments AbFeNO<sub>3</sub> and AbFeNO<sub>2</sub> were analyzed immediately when obtained.

193 Concerning the chemical analyses, concentrations of  $\text{NO}_3^-$  and  $\text{NO}_2^-$  were analyzed by  
194 high performance liquid chromatography (HPLC, WATERS 515 pump and WATERS  
195 IC-PAK ANIONS column with WATERS 432 and UV/V KONTRON detectors).  
196 Exceptionally, in the AbFeNO<sub>2</sub> experiments,  $\text{NO}_2^-$  concentration was calculated from  
197 the isotope ratio mass spectrometer (IRMS) peak areas results. Due to the high abiotic  
198  $\text{NO}_2^-$  reduction rates,  $\text{NO}_2^-$  reduction to  $\text{N}_2\text{O}$  by a sodium azide solution with acetic acid  
199 (McIlvin and Altabet, 2005; Ryabenko et al., 2009) immediately after samples  
200 collection, followed by IRMS analysis, provided a reliable method to ensure that  $\text{NO}_2^-$   
201 was not further reduced or oxidized to  $\text{NO}_3^-$  during preservation or lag time needed for  
202 other methods (such as HPLC). The  $\text{NH}_4^+$  concentration was determined by  
203 spectrophotometry (CARY 1E UV-visible) using the indophenol blue method (AbFeNO<sub>2</sub>  
204 experiments) (Bolleter et al., 1961) or by ionic chromatography (BioSedGW and  
205 BloSedDIW experiments). The  $\text{N}_2\text{O}$  accumulated at the head-space of the vials was  
206 measured by gas chromatography (GC) with an electron capture detector (ECD)  
207 (Thermo Scientific, Trace 1300). The NPDOC was analyzed by organic matter  
208 combustion (TOC 500 SHIMADZU). The dissolved Fe and trace elements were

1  
2  
3  
4  
5  
6  
7  
8  
9  
10  
11  
12  
13  
14  
15  
16  
17  
18  
19  
20  
21  
22  
23  
24  
25  
26  
27  
28  
29  
30  
31  
32  
33  
34  
35  
36  
37  
38  
39  
40  
41  
42  
43  
44  
45  
46  
47  
48  
49  
50  
51  
52  
53  
54  
55  
56  
57  
58  
59  
60  
61  
62  
63  
64  
65

209 determined by inductively coupled plasma optical emission spectrometry (ICP-OES,  
210 Perkin Elmer Optima 8300 and Perkin Elmer Optima 3200 RL).

211 The  $\delta^{15}\text{N-NO}_3^-$ ,  $\delta^{18}\text{O-NO}_3^-$  and  $\delta^{15}\text{N-NO}_2^-$  compositions were determined following the  
212 cadmium and azide reduction methods (McIlvin and Altabet, 2005; Ryabenko et al.,  
213 2009). The first step of this method consists on  $\text{NO}_3^-$  reduction to  $\text{NO}_2^-$  in columns filled  
214 with cadmium pearls. The second step consists on  $\text{NO}_2^-$  reduction to  $\text{N}_2\text{O}$  in crimp  
215 sealed vials, in which a sodium azide solution with acetic acid is added. The isotopic  
216 composition of the generated  $\text{N}_2\text{O}$  through this method or collected from the headspace  
217 of the microcosms was analyzed using a Pre-Con (Thermo Scientific) coupled to an  
218 IRMS (Finnigan MAT 253, Thermo Scientific). Notation is expressed in terms of  $\delta$  (‰)  
219 relative to the international standards: Atmospheric  $\text{N}_2$  (AIR) for  $\delta^{15}\text{N}$  and Vienna  
220 Standard Mean Oceanic Water (V-SMOW) for  $\delta^{18}\text{O}$ . Hence,  $\delta = (\text{R}_{\text{sample}} -$   
221  $\text{R}_{\text{standard}})/\text{R}_{\text{standard}}$ , where R is the ratio between the heavy and the light isotopes.  
222 According to Coplen (2011), several international and laboratory (UB) standards were  
223 interspersed among samples for normalization of the results: USGS-51, USGS-32,  
224 USGS-34, USGS-35, UB- $\text{NaNO}_3$  ( $\delta^{15}\text{N} = +16.9$  ‰,  $\delta^{18}\text{O} = +28.5$  ‰) and UB- $\text{KNO}_2$   
225 ( $\delta^{15}\text{N} = +28.5$  ‰). The reproducibility ( $1\sigma$ ) of the samples, calculated from the  
226 standards systematically interspersed in the analytical batches, was  $\pm 1.0$  ‰ for  $\delta^{15}\text{N-}$   
227  $\text{NO}_3^-$ ,  $\pm 1.5$  ‰ for  $\delta^{18}\text{O-NO}_3^-$ ,  $\pm 0.5$  for  $\delta^{18}\text{O-NO}_2^-$  and  $\pm 0.1$  for  $\delta^{15}\text{N-NO}_2^-$ .

228 Chemical and isotopic analyses were prepared at the laboratory of the MAiMA-UB  
229 research group and analyzed at the Centres Científics i Tecnològics of the Universitat  
230 de Barcelona (CCiT-UB).

### 231 *2.3. Isotopic fractionation calculation*

232 Under closed system conditions, the isotopic fractionation ( $\epsilon^{18}\text{O}$  and  $\epsilon^{15}\text{N}$ ) can be  
233 calculated by means of a Rayleigh distillation equation (**Equation 1**) (Böttcher et al.,  
234 1990; Mariotti et al., 1988). Thus,  $\epsilon$  can be obtained from the slope of the linear

235 correlation between the natural logarithm of the substrate remaining fraction  
236 ( $\ln(C_{\text{residual}}/C_{\text{initial}})$ , where C refers to analyte concentration) and the determined isotope  
237 ratios ( $\ln(R_{\text{residual}}/R_{\text{initial}})$ , where  $R = (\delta+1)$ ).

$$\ln \left( \frac{R_{\text{residual}}}{R_{\text{initial}}} \right) = \epsilon \times \ln \left( \frac{C_{\text{residual}}}{C_{\text{initial}}} \right) \text{ Equation 1}$$

### 240 3. RESULTS AND DISCUSSION

241 All data obtained from the laboratory experiments is reported in the Supporting  
242 Information **Table S2**.

#### 243 3.1. Microbial $\text{NO}_3^-$ reduction by Fe(II)-containing minerals

244 During the first week of incubation, in the microbial experiments containing  
245 groundwater or deionized water with  $\text{NO}_3^-$ , plus sediment, plus minerals (BioSedGW-  
246 Min and BioSedDIW-Min), the  $\text{NO}_3^-$  concentration decreased by 30-60 % of the initial  
247 values (**Figures 1A and 1B**). Attenuation of  $\text{NO}_3^-$  was also observed in the BioSedGW-  
248 C microcosms that lacked mineral (up to 40 %  $\text{NO}_3^-$  reduction). Therefore, the  
249 beginning of denitrification was likely caused by heterotrophic bacteria that used the  
250 organic C from both sediment and groundwater as electron donor. In blank  
251 experiments containing only MilliQ water and sediment,  $0.4 \pm 0.03$  mM NPDOC leaked  
252 from this sediment, which has to be added to the 0.2 mM NPDOC already present in  
253 groundwater in the BioSedGW experiments. At the beginning of microbial  $\text{NO}_3^-$   
254 reduction,  $\text{NO}_2^-$  usually accumulates until bacterial communities adapt to the new redox  
255 conditions caused by the electron donor addition. This can be explained by an earlier  
256 induction of  $\text{NO}_3^-$  reductases with respect to  $\text{NO}_2^-$  reductases that could provoke lower  
257 initial  $\text{NO}_2^-$  reduction rates. Hence, the main parameters affecting  $\text{NO}_2^-$  accumulation  
258 are the initial inoculum, the type of electron donor involved and its molar ratio with  
259 respect to  $\text{NO}_3^-$  (Akunna et al., 1993; Betlach and Tiedje, 1981; Ge et al., 2012; Zumft,

1  
2  
3  
4  
5  
6  
7  
8  
9  
10  
11  
12  
13  
14  
15  
16  
17  
18  
19  
20  
21  
22  
23  
24  
25  
26  
27  
28  
29  
30  
31  
32  
33  
34  
35  
36  
37  
38  
39  
40  
41  
42  
43  
44  
45  
46  
47  
48  
49  
50  
51  
52  
53  
54  
55  
56  
57  
58  
59  
60  
61  
62  
63  
64  
65

1997). The lower  $\text{NO}_2^-$  accumulation found in BioSedGW-Min microcosms (up to 0.2 mM) compared to BioSedDIW-Min microcosms (up to 0.6 mM) is therefore consistent with a higher NPDOC content and inoculum in BioSedGW (groundwater + sediment) compared to BioSedDIW microcosms (just sediment) (**Figures 1C and 1D**).

After the first week,  $\text{NO}_3^-$  or  $\text{NO}_2^-$  concentrations did not change significantly in the BioSedDIW experiments (**Figures 1B and 1D**). In the BioSedGW microcosms with micro-sized (Mag, Ol, Sd) or lacking minerals (C), significant differences in  $\text{NO}_3^-$  concentration were not observed (**Figure 1A**), but from day 118 on,  $\text{NO}_2^-$  was no longer detected (**Figure 1C**). These results suggested that organic C from sediment and groundwater and available Fe(II) from micro-sized minerals were insufficient to complete  $\text{NO}_3^-$  reduction to  $\text{N}_2$ . Also, that the higher microbial inoculum and dissolved organic C content in BioSedGW experiments allowed an extended progression of the reaction compared to BioSedDIW experiments. In contrast, in the BioSedGW-Mag-NP microcosms, about 96 %  $\text{NO}_3^-$  reduction was achieved in 91 days (**Figure 1A**), showing transient  $\text{NO}_2^-$  accumulation (up to 0.2 mM) until day 91 (**Figure 1C**). In the BioSedGW microcosms,  $\text{NH}_4^+$  concentration was below 0.04 mM, discarding a major contribution of dissimilatory  $\text{NO}_3^-$  reduction to ammonium (DNRA) and suggesting that the end products of  $\text{NO}_3^-$  reduction were gaseous N compounds. The measured  $\text{N}_2\text{O}$  at the head-space of the BioSedGW vials was below 0.1 % of the initial N in the control, below 0.4 % in the micro-sized minerals microcosms, and below 0.8 % in the Mag-NP microcosms. The highest concentration being detected in the BioSedGW-Mag-NP microcosms is consistent with the highest reduction being observed in these batches. The low percentage of N in form of  $\text{N}_2\text{O}$  found in the BioSedGW experiments suggested that the final gaseous product of the microbial  $\text{NO}_3^-$  reduction was  $\text{N}_2$ , either during the initial heterotrophic activity and as a result of the denitrification stimulated by Mag-NP. Therefore, if during the denitrification stimulated by Mag-NP, an abiotic reactivity between  $\text{NO}_2^-$  and the available Fe(II) occurred, the produced  $\text{N}_2\text{O}$  seemed to

1  
2  
3  
4  
5  
6  
7  
8  
9  
10  
11  
12  
13  
14  
15  
16  
17  
18  
19  
20  
21  
22  
23  
24  
25  
26  
27  
28  
29  
30  
31  
32  
33  
34  
35  
36  
37  
38  
39  
40  
41  
42  
43  
44  
45  
46  
47  
48  
49  
50  
51  
52  
53  
54  
55  
56  
57  
58  
59  
60  
61  
62  
63  
64  
65

287 be further reduced to  $N_2$  by microorganisms. Similarly, in a  $NO_3^-$  polluted aquifer in the  
288 presence of Fe(II) and low organic C, the results obtained by Smith et al. (2017)  
289 suggested that  $NO_3^-$  was reduced both heterotrophically and lithoautotrophically while  
290  $NO_2^-$  was also reduced abiotically and the generated  $N_2O$  was further reduced to  $N_2$  by  
291 microorganisms down-gradient.

292 Our results suggest that Mag-NP allowed a higher structural Fe(II) availability with  
293 respect to micro-sized Mag due to an increased surface area coupled to a decreased  
294 grain size (Supporting Information **Section S2**). Similar to our results, Aquilina et al.  
295 (2018) and Yang et al. (2017) related an increased denitrification rate to a decreased  
296 grain size of minerals (granite-biotite and pyrothite, respectively). Smaller particles  
297 usually enhance mineral solubility, which might accelerate microbial reduction rates.  
298 Braunschweig et al. (2013) even suggested that in case of nanoparticles precipitation,  
299 the solubility might be independent of the aggregate size. However, dissolved  $Fe^{2+}$   
300 concentration was below detection limit in almost all samples of our microbial  
301 experiments. Bacteria likely oxidized either structural Fe(II) or adsorbed Fe(II) on  
302 mineral surface. Alternatively, if  $Fe^{2+}$  was released through dissolution, bacteria  
303 immediately oxidized it to Fe(III), which precipitated and became unavailable for  
304 detection. The ICP results (Supporting Information **Table S2.2**), neither proved a  
305 possible mineral dissolution. The Mag Fe(II)/Fe(III) stoichiometry can also influence its  
306 reactivity (Gorski et al., 2010). Nevertheless, during the protocol followed to obtain  
307 nano-sized from micro-sized Mag we did not expect a variation in the Fe(II)/Fe(III) ratio  
308 (Supporting Information **Section S2**). Hence, we discarded this factor as a main  
309 contributor for the observed changes in reactivity between the two different Mag grain  
310 sizes tested in our experiments. On the other hand, considering that not all structural  
311 Fe(II) was available for reduction, the Fe(II)/N molar ratio in the micro-sized minerals  
312 experiments was likely too low to complete  $NO_3^-$  reduction, especially in the case of Sd  
313 and OI (initial Fe(II)/N of 13 and 7, respectively compared to 24 calculated for Mag and

1  
2  
3  
4  
5  
6  
7  
8  
9  
10  
11  
12  
13  
14  
15  
16  
17  
18  
19  
20  
21  
22  
23  
24  
25  
26  
27  
28  
29  
30  
31  
32  
33  
34  
35  
36  
37  
38  
39  
40  
41  
42  
43  
44  
45  
46  
47  
48  
49  
50  
51  
52  
53  
54  
55  
56  
57  
58  
59  
60  
61  
62  
63  
64  
65

314 Mag-NP). In a study with *Microbacterium* sp. W5, 90 % NO<sub>3</sub><sup>-</sup> removal was achieved  
315 when using a Fe(II)/N ratio of nearly 30, which is far above from the stoichiometric ratio  
316 of 5 (Zhou et al., 2016).

317 In a previous study, in groundwater collected from the SMC-002 well, Hernández-del  
318 Amo et al. (2018) identified at genus level *Sideroxydans*, *Acidiferrobacter* and  
319 *Thiobacillus* species, which are capable of Fe(II) oxidation and NO<sub>3</sub><sup>-</sup> reduction, and  
320 *Nitrospira*, *Geobacillus* and *Solitalea* species, which are also capable to reduce NO<sub>3</sub><sup>-</sup>.  
321 Bacterial species involved in these genera could have stimulated the NO<sub>3</sub><sup>-</sup> reduction  
322 observed in the BioSedGW experiments since groundwater collected from the same  
323 well was employed. The microbial NO<sub>3</sub><sup>-</sup> dependent Fe(II) oxidation (NDFO)  
324 mechanisms, are not still completely understood (Bryce et al., 2018; Price et al., 2018;  
325 Straub et al., 1996). Among the microorganisms that have been related to NDFO,  
326 lithoautotrophs have been identified but most of them are mixotrophic, requiring an  
327 organic C co-substrate for growth, or even the NDFO can result from a synergistic  
328 activity between different NO<sub>3</sub><sup>-</sup> reducing and Fe(II) oxidizing microorganisms (Bryce et  
329 al., 2018; Melton et al., 2014; Price et al., 2018; Weber et al., 2006). Some authors  
330 propose that NDFO mixotrophic communities might need a lower organic C supply to  
331 reduce NO<sub>3</sub><sup>-</sup> compared to heterotrophic communities (Devlin et al., 2000; He et al.,  
332 2016). Hence, we could not discard the simultaneous use of organic C from sediment  
333 and groundwater and Fe(II) from minerals in our microbial experiments with Mag-NP,  
334 Mag, Ol or Sd.

### 335 3.2. NO<sub>3</sub><sup>-</sup> and NO<sub>2</sub><sup>-</sup> abiotic reactivity with Fe(II)

336 The abiotic experiments containing synthetic water with NO<sub>3</sub><sup>-</sup> and dissolved Fe<sup>2+</sup> plus  
337 micro-sized Mag, Ol or Sd (AbFeNO<sub>3</sub>) showed a lack of significant reactivity (**Figure**  
338 **2A**). This lack of reactivity was also observed in qualitative previous tests performed  
339 with NO<sub>3</sub><sup>-</sup> and the micro-sized minerals without addition of dissolved Fe<sup>2+</sup> (Supporting

1  
2  
3  
4  
5  
6  
7  
8  
9  
10  
11  
12  
13  
14  
15  
16  
17  
18  
19  
20  
21  
22  
23  
24  
25  
26  
27  
28  
29  
30  
31  
32  
33  
34  
35  
36  
37  
38  
39  
40  
41  
42  
43  
44  
45  
46  
47  
48  
49  
50  
51  
52  
53  
54  
55  
56  
57  
58  
59  
60  
61  
62  
63  
64  
65

340 Information **Table S2.8**). These results reinforced that the  $\text{NO}_3^-$  reduction observed in  
341 our microbial experiments (BioSedGW and BioSedDIW) was caused by biological  
342 activity.

343 The abiotic experiments containing synthetic water with  $\text{NO}_2^-$  plus the micro-sized Mag,  
344 Ol and Sd (Ab $\text{NO}_2$ ) also showed a lack of significant reactivity (**Figure 2B**). However, a  
345 rapid  $\text{NO}_2^-$  reduction was observed in the abiotic experiments containing synthetic  
346 water with  $\text{NO}_2^-$  and dissolved  $\text{Fe}^{2+}$  involving the lack (C) or addition of the micro-sized  
347 Mag, Ol and Sd (Ab $\text{FeNO}_2$ ) (**Figure 3A**). The beginning of the reaction seemed to be  
348 immediate and  $\text{NO}_2^-$  removal was completed in both the Ab $\text{FeNO}_2$ -Min and Ab $\text{FeNO}_2$ -C  
349 experiments, which is consistent with previous studies showing a significant  $\text{NO}_2^-$   
350 reduction (approximately 60 % in 4 days) even at an equimolar dissolved  $\text{Fe}^{2+}/\text{NO}_2^-$   
351 molar ratio (Jones et al., 2015). A faster reduction (~ 50 hours) was observed in the  
352 experiments containing Sd compared to those without mineral or with Mag or Ol (~ 175  
353 hours), possibly due to an increased Fe(II) availability in Sd. Since the measured  $\text{NH}_4^+$   
354 was below 0.05 mM, it was considered that  $\text{NO}_2^-$  was reduced to gaseous products. As  
355 previously observed by other authors,  $\text{N}_2\text{O}$  accumulated at the headspace of the  
356 batches as a result of the  $\text{NO}_2^-$  abiotic reduction by Fe(II) oxidation (Buchwald et al.,  
357 2016; Chen et al., 2018; Coby and Picardal, 2005; Wang et al., 2016). Our results point  
358 that  $\text{N}_2\text{O}$  was the end product because a mass balance between the remaining  $\text{NO}_2^-$  in  
359 the solution and the accumulated  $\text{N}_2\text{O}$  in the headspace for each vial was close to the  
360  $\text{NO}_2^-$  initial value (**Figure 3B**). Kampschreur et al. (2011) observed a complete recovery  
361 of  $\text{NO}_2^-$  as NO and  $\text{N}_2\text{O}$ . Hence, the missing mass balance complement to  $\text{N}_2\text{O}$  is likely  
362 to be found as NO. According to these results, if Fe(II)-containing minerals are applied  
363 in polluted water bodies to promote denitrification,  $\text{NO}_2^-$  accumulation could be avoided  
364 after its abiotic reduction in the presence of dissolved  $\text{Fe}^{2+}$ . However, this  $\text{NO}_2^-$  abiotic  
365 reduction would be beneficial only if the generated  $\text{N}_2\text{O}$  is further reduced by  
366 microorganisms.



1  
2  
3  
4  
5  
6  
7  
8  
9  
10  
11  
12  
13  
14  
15  
16  
17  
18  
19  
20  
21  
22  
23  
24  
25  
26  
27  
28  
29  
30  
31  
32  
33  
34  
35  
36  
37  
38  
39  
40  
41  
42  
43  
44  
45  
46  
47  
48  
49  
50  
51  
52  
53  
54  
55  
56  
57  
58  
59  
60  
61  
62  
63  
64  
65

367 In these AbFeNO<sub>2</sub> experiments, a dissolved Fe<sup>2+</sup> decrease was observed in  
368 accordance to NO<sub>2</sub><sup>-</sup> reduction from the initial 5 mM to approximately 2 mM, showing no  
369 significant differences between the experiment without mineral or the ones with micro-  
370 sized Mag, Ol or Sd (**Figure 3C**). Total dissolved Fe measured by ICP-OES was  
371 considered to be solely dissolved Fe<sup>2+</sup> since Fe(III) was quickly precipitated and  
372 because the ICP-OES method have previously shown equal results compared with  
373 ferrozine analysis (Smith et al., 2017). In studies focusing on the abiotic NO<sub>2</sub><sup>-</sup> reduction  
374 coupled to Fe(II) oxidation, homogeneous reactions produced by oxidation of dissolved  
375 Fe<sup>2+</sup> are distinguished from heterogeneous reactions in which Fe(II) is associated to  
376 mineral or bacterial surfaces or found as structural Fe(II) within minerals. Some studies  
377 suggest that a faster NO<sub>2</sub><sup>-</sup> reduction is produced through the heterogeneous reaction  
378 (Buchwald et al., 2016; Dhakal et al., 2013) although low or null dissolved Fe<sup>2+</sup>  
379 concentrations can inhibit NO<sub>2</sub><sup>-</sup> reduction even in the presence of mineral-associated  
380 Fe(II) (Tai and Dempsey, 2009). This is consistent with the lack of reactivity found for  
381 the AbNO<sub>2</sub> compared to the AbFeNO<sub>2</sub> experiments.

### 382 *3.3. Isotopic characterization*

#### 383 *3.3.1. Isotopic fractionation of NO<sub>3</sub><sup>-</sup> during microbial reduction*

384 The initial isotopic values measured in groundwater of +11.3 ‰ for δ<sup>15</sup>N-NO<sub>3</sub><sup>-</sup> and  
385 +10.1 ‰ for δ<sup>18</sup>O-NO<sub>3</sub><sup>-</sup> increased to +158.1 ‰ and +47.5 ‰, respectively, throughout  
386 the microbial NO<sub>3</sub><sup>-</sup> reduction stimulated by the Mag-NP (BioSedGW-Mag-NP). The  
387 calculated ε<sup>15</sup>N<sub>NO3</sub> was -33.1 ‰ (R<sup>2</sup> = 0.86) and ε<sup>18</sup>O<sub>NO3</sub> was -10.7 ‰ (R<sup>2</sup> = 0.74)  
388 (**Figure 4A**), giving a ε<sup>15</sup>N<sub>NO3</sub>/ε<sup>18</sup>O<sub>NO3</sub> of 3.1. While this ε<sup>18</sup>O<sub>NO3</sub> is within the range of  
389 values reported for microbial denitrification experiments at laboratory-scale, the ε<sup>15</sup>N<sub>NO3</sub>  
390 and the ε<sup>15</sup>N<sub>NO3</sub>/ε<sup>18</sup>O<sub>NO3</sub> are found in the highest extreme (absolute values) (see **Table**  
391 **2**). Similar ε<sup>15</sup>N<sub>NO3</sub> were reported by Torrentó et al. (2011) in batch experiments using  
392 aquifer material and pyrite (-27.6 ‰) and by Tsushima et al. (2006) in column



393 experiments using riparian aquifer sediments (-34.1 ‰). However, Torrentó et al.  
394 (2011) obtained a  $\epsilon^{15}\text{N}_{\text{NO}_3}/\epsilon^{18}\text{O}_{\text{NO}_3}$  close to 1 and Tsushima et al. (2006) did not report  
395 values for  $\epsilon^{18}\text{O}_{\text{NO}_3}$ . Likely due to  $\delta^{18}\text{O}\text{-NO}_2^-$  equilibration with  $\delta^{18}\text{O}\text{-H}_2\text{O}$  and subsequent  
396  $\text{NO}_2^-$  reoxidation to  $\text{NO}_3^-$ , Knöller et al. (2011) found a  $\epsilon^{15}\text{N}_{\text{NO}_3}/\epsilon^{18}\text{O}_{\text{NO}_3}$  of 3 ( $\epsilon^{15}\text{N}_{\text{NO}_3} = -$   
397 16.2 ‰ and  $\epsilon^{18}\text{O}_{\text{NO}_3} = -5.5$  ‰), using succinate as electron donor and *Pseudomonas*  
398 *pseudoalcaligenes*. These results might be coherent with our results after such a long  
399 incubation and important  $\text{NO}_2^-$  accumulation. After  $\delta^{18}\text{O}\text{-NO}_2^-$  exchange with  $\delta^{18}\text{O}\text{-H}_2\text{O}$ ,  
400 which ranges between -4 and -7 ‰ in the area where the SMC-002 well is placed, if  
401  $\text{NO}_2^-$  reoxidates to  $\text{NO}_3^-$ , a decreased  $\delta^{18}\text{O}\text{-NO}_3^-$  enrichment might be expected  
402 compared to the  $\delta^{15}\text{N}\text{-NO}_3^-$  enrichment. Therefore, the resulting  $\epsilon^{15}\text{N}_{\text{NO}_3}/\epsilon^{18}\text{O}_{\text{NO}_3}$  might  
403 be higher than those close to 1.0 usually resulting from  $\text{NO}_3^-$  reduction to  $\text{NO}_2^-$  and  
404 subsequent reduction to gaseous products. If a bioremediation strategy by using Mag-  
405 NP to promote denitrification is implemented, the calculated  $\epsilon$  values in the present  
406 study could be applied to evaluate the efficiency of the treatment (Margalef-Martí et al.,  
407 2019c; Meckenstock et al., 2004; Vidal-Gavilan et al., 2013). However, due to the  $\delta^{18}\text{O}\text{-}$   
408  $\text{NO}_2^-$  exchange with  $\delta^{18}\text{O}\text{-H}_2\text{O}$ , calculations derived from  $\epsilon^{18}\text{O}_{\text{NO}_3}$  might be used with  
409 caution.

410 In the case of the microbial experiments containing micro-sized minerals (BioSedGW-  
411 Mag/OI/Sd), an isotopic fractionation during the initial incomplete denitrification was  
412 also observed. These isotopic results are presented as a whole since a similar trend  
413 was found for the different tested conditions, which is explained by the use of NPDOC  
414 released from sediment and groundwater as electron donor in all cases. Calculated  
415  $\epsilon^{15}\text{N}_{\text{NO}_3}$  was -12.0 ‰ ( $R^2 = 0.56$ ) and  $\epsilon^{18}\text{O}_{\text{NO}_3}$  was -10.9 ‰ ( $R^2 = 0.63$ ) (**Figure 4B and**  
416 **4D**), giving a  $\epsilon^{15}\text{N}_{\text{NO}_3}/\epsilon^{18}\text{O}_{\text{NO}_3}$  of 1.1. These values are within the range reported for  
417 microbial denitrification in laboratory-scale experiments (see **Table 2**) and point to a  
418 lack of  $\text{NO}_2^-$  reoxidation in contrast to the Mag-NP experiments. The main reason for  
419 the  $\text{NO}_2^-$  reoxidation occurrence only in the Mag-NP experiments could be the longer

1  
2  
3  
4  
5  
6  
7  
8  
9  
10  
11  
12  
13  
14  
15  
16  
17  
18  
19  
20  
21  
22  
23  
24  
25  
26  
27  
28  
29  
30  
31  
32  
33  
34  
35  
36  
37  
38  
39  
40  
41  
42  
43  
44  
45  
46  
47  
48  
49  
50  
51  
52  
53  
54  
55  
56  
57  
58  
59  
60  
61  
62  
63  
64  
65

420 incubation time and therefore, longer persistence of  $\text{NO}_2^-$  accumulation. This long  
421 persistence of  $\text{NO}_2^-$  could have let enough time for activation of the enzymatic  $\text{NO}_2^-$   
422 oxidation. In the groundwater employed for the experiments, bacterial species from the  
423 genus *Nitrospira* were identified (Hernández-del Amo et al., 2018). Microorganisms  
424 from this genus have been previously related to both nitrification and denitrification  
425 activity and could have allowed both  $\text{NO}_2^-$  reduction and oxidation (Koch et al., 2015).

### 426 3.3.2. Isotopic fractionation of $\text{N-NO}_2^-$ during the abiotic reduction

427 In the abiotic  $\text{NO}_2^-$  reduction experiments with dissolved  $\text{Fe}^{2+}$  with or without micro-  
428 sized minerals ( $\text{AbFeNO}_2$ ), the initial  $\delta^{15}\text{N-NO}_2^-$  of -28.5 ‰ increased to -16.8 ‰, -14.9  
429 ‰, -14.5 ‰ and +7.1 ‰ in the C, Mag, Sd and OI batches, respectively. No significant  
430 differences were observed in the calculated  $\epsilon^{15}\text{N}_{\text{NO}_2}$  for these experiments (**Figure 4C**),  
431 suggesting that the observed  $\text{NO}_2^-$  abiotic reduction was mainly caused by dissolved  
432  $\text{Fe}^{2+}$  oxidation. The  $\epsilon^{15}\text{N}_{\text{NO}_2}$  values were -14.1 ‰ ( $R^2 = 0.92$ ) for the  $\text{AbFeNO}_2\text{-C}$ , -14.1  
433 ‰ ( $R^2 = 0.99$ ) for Sd, -14.6 ‰ ( $R^2 = 0.89$ ) for Mag and -17.8 ‰ ( $R^2 = 0.95$ ) for OI. In  
434 these experiments, the  $\epsilon^{18}\text{O}_{\text{NO}_2}$  was not calculated because no clear  $\delta^{18}\text{O-NO}_2^-$   
435 enrichment coupled to  $\text{NO}_2^-$  reduction was observed, pointing to  $\delta^{18}\text{O-NO}_2^-$  equilibration  
436 with  $\delta^{18}\text{O-H}_2\text{O}$ . In similar studies, a possible contribution from  $\delta^{18}\text{O-NO}_2^-$  equilibration  
437 with  $\delta^{18}\text{O-H}_2\text{O}$  could not be discarded (Buchwald et al., 2016; Grabb et al., 2017), and  
438 Jones et al. (2015) also found a weaker  $\delta^{18}\text{O-NO}_2^-$  enrichment compared to the  $\delta^{15}\text{N-}$   
439  $\text{NO}_2^-$  enrichment ( $\epsilon^{18}\text{O}_{\text{NO}_2} = 10$  ‰ vs  $\epsilon^{15}\text{N}_{\text{NO}_2} = 13$  ‰, respectively). These authors  
440 proposed an exchange between  $\delta^{18}\text{O-NO}_2^-$  and  $\delta^{18}\text{O-H}_2\text{O}$  since de  $\delta^{18}\text{O-NO}_2^-$   
441 continued to variate after the abiotic  $\text{NO}_2^-$  reduction was stopped.

442 Testing the  $\text{NO}_2^-$  abiotic reduction with different incubation conditions, other authors  
443 have reported  $\epsilon^{15}\text{N}_{\text{NO}_2}$  values ranging from -2.3 ‰ to -44.8 ‰,  $\epsilon^{18}\text{O}_{\text{NO}_2}$  from -4.1 ‰ to -  
444 33.0 ‰, and  $\epsilon^{15}\text{N}_{\text{NO}_2}/\epsilon^{18}\text{O}_{\text{NO}_2}$  between 0.5 and 1.6 (see **Table 2**). Our  $\epsilon^{15}\text{N}_{\text{NO}_2}$  results fall  
445 within this wide range. Although different isotopic trends were found between  $\text{NO}_2^-$

1  
2  
3  
4  
5  
6  
7  
8  
9  
10  
11  
12  
13  
14  
15  
16  
17  
18  
19  
20  
21  
22  
23  
24  
25  
26  
27  
28  
29  
30  
31  
32  
33  
34  
35  
36  
37  
38  
39  
40  
41  
42  
43  
44  
45  
46  
47  
48  
49  
50  
51  
52  
53  
54  
55  
56  
57  
58  
59  
60  
61  
62  
63  
64  
65

446 reduction caused by structural Fe(II) or Fe(II) adsorbed onto mineral surfaces or  
447 dissolved Fe<sup>2+</sup> in the laboratory studies performed by Buchwald et al. (2016) and Grabb  
448 et al. (2017), we did not observe such difference. Considering the wide range of  
449 reported  $\epsilon$  values, it is not likely that the NO<sub>2</sub><sup>-</sup> isotopic characterization could be useful  
450 at field-scale to distinguish the homogeneous and heterogeneous reactions.  
451 Furthermore,  $\epsilon^{15}\text{N}_{\text{NO}_2}$  and  $\epsilon^{18}\text{O}_{\text{NO}_2}$  within this range have also been reported for the  
452 microbial NO<sub>2</sub><sup>-</sup> reduction, which resulted in  $\epsilon^{15}\text{N}_{\text{NO}_2}/\epsilon^{18}\text{O}_{\text{NO}_2}$  between 0.7 and 22.0 (see  
453 **Table 2**). Therefore, the NO<sub>2</sub><sup>-</sup> isotopic characterization may neither be useful at field-  
454 scale to distinguish the abiotic from the microbial NO<sub>2</sub><sup>-</sup> reduction.

### 455 *3.3.3. Isotopic evolution of N<sub>2</sub>O in microbial and abiotic experiments*

456 The isotopic composition of the accumulated N<sub>2</sub>O in the microbial NO<sub>3</sub><sup>-</sup> reduction  
457 experiments showed variations. Neither N<sub>2</sub>O nor NO<sub>3</sub><sup>-</sup> concentrations presented a clear  
458 relationship with the determined  $\delta^{15}\text{N-N}_2\text{O}$  or  $\delta^{18}\text{O-N}_2\text{O}$  due to the simultaneous  
459 production and reduction of this intermediate product of denitrification. However, a  
460 correlation was observed between  $\delta^{18}\text{O-N}_2\text{O}$  and  $\delta^{15}\text{N-N}_2\text{O}$ , giving slopes ranging from  
461 -2.4 to +2.3 for the BioSedGW-Min experiments (**Figures 5A and 5B**). Given the lack  
462 of studies reporting an exhaustive isotopic characterization of nitrous oxide during the  
463 autotrophic denitrification, we don't have consistent hypothesis to explain why the  
464 micro-sized Mag gave an inverse slope compared to OI and Sd. We think that the  
465 isotopic characterization of N<sub>2</sub>O during its simultaneous production and reduction  
466 during denitrification require further investigation.

467 The  $\delta^{15}\text{N-N}_2\text{O}$  ranged from -11.1 ‰ to +63.4 ‰ and the  $\delta^{18}\text{O-N}_2\text{O}$  from -3.5 ‰ to +62.6  
468 ‰ in the BioSedGw-Mag-NP experiments, while in the BioSedGW experiments  
469 containing micro-sized minerals, the  $\delta^{15}\text{N-N}_2\text{O}$  ranged from -31.3 ‰ to +5.1 ‰ and the  
470  $\delta^{18}\text{O-N}_2\text{O}$  from -12.0 ‰ to +52.4 ‰. The increased variation of the  $\delta^{15}\text{N-N}_2\text{O}$  in the  
471 BioSedGw-Mag-NP compared to the BioSedGW-Mag/OI/Sd and the similar  $\delta^{18}\text{O-N}_2\text{O}$

1  
2  
3  
4  
5  
6  
7  
8  
9  
10  
11  
12  
13  
14  
15  
16  
17  
18  
19  
20  
21  
22  
23  
24  
25  
26  
27  
28  
29  
30  
31  
32  
33  
34  
35  
36  
37  
38  
39  
40  
41  
42  
43  
44  
45  
46  
47  
48  
49  
50  
51  
52  
53  
54  
55  
56  
57  
58  
59  
60  
61  
62  
63  
64  
65

472 enrichment between the BioSedGw-Mag-NP and the BioSedGW-Mag/OI/Sd, is  
473 consistent with the obtained  $\epsilon$  values for the substrates. Moving to the abiotic  
474 experiments with dissolved  $\text{Fe}^{2+}$  with or without micro-sized minerals ( $\text{AbFeNO}_2$ ), a  
475 lower variation in the  $\delta^{15}\text{N-N}_2\text{O}$  was observed compared to the microbial experiments  
476 (**Figure 5C**). In these abiotic experiments, it is likely that during the beginning of  $\text{N}_2\text{O}$   
477 production the  $\delta^{15}\text{N-N}_2\text{O}$  decreases and afterwards increases (e.g. initial  $\text{N}_2\text{O}$  produced  
478 in the  $\text{AbFeNO}_2$ -Mag experiments presents a  $\delta^{15}\text{N-N}_2\text{O}$  of -48.4 ‰ that decreases to -  
479 53.8 ‰ and then increases to -43.4 ‰). Because the  $\delta^{18}\text{O-NO}_2^-$  in these experiments  
480 presented equilibration with  $\delta^{18}\text{O-H}_2\text{O}$ , the  $\delta^{18}\text{O-N}_2\text{O}$  results did not provide valuable  
481 information.

482 Since a much higher  $\delta^{15}\text{N-N}_2\text{O}$  variation was observed for the microbial experiments  
483 compared to the abiotic experiments, observing important  $\delta^{15}\text{N-N}_2\text{O}$  variations in  
484 denitrification studies could be indicative of microbial activity. Chen et al. (2018) also  
485 observed a higher increase of  $\delta^{15}\text{N-N}_2\text{O}$  in microbial compared to abiotic  $\text{NO}_2^-$   
486 reduction experiments. An alternative way to use the  $\delta^{15}\text{N-N}_2\text{O}$  data to distinguish  
487 microbial and abiotic reactions could be modelling the substrate ( $\text{NO}_3^-$  or  $\text{NO}_2^-$ ) and  
488 product ( $\text{N}_2\text{O}$ )  $\delta^{15}\text{N}$  composition by applying the calculated  $\epsilon^{15}\text{N}_{\text{NO}_3}$  and  $\epsilon^{15}\text{N}_{\text{NO}_2}$  in batch  
489 experiments and to compare it with the determined  $\delta^{15}\text{N}$  in the samples (Mariotti et al.,  
490 1981). Since  $\text{N}_2\text{O}$  is an intermediate product of the  $\text{NO}_3^-$  microbial reduction but the end  
491 product of the abiotic  $\text{NO}_2^-$  reduction, at the end of the reaction, the determined  $\delta^{15}\text{N-N}_2\text{O}$   
492  $\text{N}_2\text{O}$  of the samples should fit the initial  $\delta^{15}\text{N}$  of the substrate in the case of the  $\text{NO}_2^-$   
493 abiotic reduction but should be higher than that in the case of the  $\text{NO}_3^-$  microbial  
494 reduction. For the microbial experiments with Mag-NP (BioSedGW-Mag-NP), the  
495 determined  $\delta^{15}\text{N-N}_2\text{O}$  in most of the samples was above the modelled line, indicating a  
496 further reduction of the  $\text{N}_2\text{O}$  to  $\text{N}_2$  (**Figure 6**). Contrarily, in the abiotic experiments with  
497 dissolved  $\text{Fe}^{2+}$  with or without micro-sized minerals ( $\text{AbFeNO}_2$ ), the  $\delta^{15}\text{N-N}_2\text{O}$  of the  
498 samples presented a tendency towards the substrate initial  $\delta^{15}\text{N}$  at the end of the

1  
2  
3  
4  
5  
6  
7  
8  
9  
10  
11  
12  
13  
14  
15  
16  
17  
18  
19  
20  
21  
22  
23  
24  
25  
26  
27  
28  
29  
30  
31  
32  
33  
34  
35  
36  
37  
38  
39  
40  
41  
42  
43  
44  
45  
46  
47  
48  
49  
50  
51  
52  
53  
54  
55  
56  
57  
58  
59  
60  
61  
62  
63  
64  
65

499 reaction, confirming that N<sub>2</sub>O was the end product of the NO<sub>2</sub><sup>-</sup> abiotic reduction. The  
500 observation of some samples δ<sup>15</sup>N-N<sub>2</sub>O values below the modelled line, at the  
501 beginning of the reaction, suggested the generation of intermediate NO. Similar to our  
502 results, Chen et al. (2018) found initial δ<sup>15</sup>N-N<sub>2</sub>O more negative than the starting δ<sup>15</sup>N-  
503 NO<sub>3</sub><sup>-</sup> and δ<sup>15</sup>N-NO<sub>2</sub><sup>-</sup> due to NO generation. Also in another study, a good correlation  
504 was found between the calculated ε<sup>15</sup>N<sub>NO<sub>2</sub> and the obtained δ<sup>15</sup>N-N<sub>2</sub>O values for the  
505 abiotic NO<sub>2</sub><sup>-</sup> reduction by Fe(II) oxidation (Jones et al., 2015).</sub>

506 According to these results, the δ<sup>15</sup>N-N<sub>2</sub>O analysis is useful to determine if N<sub>2</sub>O is an  
507 intermediate or final product of N compounds reduction. To quantify the contributions of  
508 microbial and abiotic NO<sub>2</sub><sup>-</sup> reduction by Fe<sup>2+</sup> oxidation, performing new experiments to  
509 determine the ε<sup>15</sup>N<sub>NO<sub>2</sub> and the ε<sup>15</sup>N<sub>N<sub>2</sub>O</sub> in microbial experiments could be advantageous  
510 after coupling this data to the already determined ε<sup>15</sup>N<sub>NO<sub>2</sub> in abiotic experiments and  
511 ε<sup>15</sup>N<sub>NO<sub>3</sub></sub> in microbial experiments. Liu et al. (2018) assessed the contribution of each  
512 reaction by modelling the kinetics of each reaction tested separately. Concerning the  
513 Fe(II) oxidation, they found a major contribution of the abiotic compared to the  
514 microbial reaction while for the NO<sub>2</sub><sup>-</sup> reduction, they found a major contribution of the  
515 microbial compared to the abiotic reaction. However, the use of models developed  
516 either by using isotopes or isotopic data could be limited at field-scale due to the  
517 complexity of the reactions. For example, Jamieson et al. (2018) suggested that the  
518 bacterial production of exopolymeric substances (EPS) could increase the NO<sub>2</sub><sup>-</sup> abiotic  
519 reduction rate since Fe(II) can be complexed to the organic C from EPS. Other data  
520 that could be helpful in assessing the contribution of the microbial and abiotic reaction  
521 could be the analysis of the generated secondary minerals (Chen et al., 2018; Liu et  
522 al., 2018), the site preference (SP) of the generated N<sub>2</sub>O (i.e. the intramolecular  
523 distribution of N isotopes since the N<sub>2</sub>O molecule has an asymmetric linear structure  
524 (N-N-O)) (Buchwald et al., 2016; Heil et al., 2014; Jones et al., 2015) and the Fe(II)  
525 isotopic composition.</sub></sub>

526

## 527 CONCLUSIONS

528 In our microbial experiments containing groundwater and sediment plus or without  
529 minerals (BioSedGW-Mag-NP/Mag/Sd/OI/C), the beginning of denitrification was  
530 caused by heterotrophic bacteria that used organic C from sediment and/or  
531 groundwater. Afterwards, complete  $\text{NO}_3^-$  reduction to  $\text{N}_2$  was only achieved in the  
532 BioSedGW-Mag-NP microcosms, suggesting an increased Fe(II) availability of nano-  
533 sized compared to micro-sized Mag. Reactivity between the Fe(II)-containing minerals  
534 and  $\text{NO}_3^-$  or  $\text{NO}_2^-$  was negligible. However, the abiotic  $\text{NO}_2^-$  reduction to  $\text{N}_2\text{O}$  by  
535 dissolved  $\text{Fe}^{2+}$  was demonstrated both in the presence and absence of micro-sized  
536 minerals (AbFeNO<sub>2</sub>-Mag/Sd/OI/C).

537 For the BioSedGW-Mag-NP experiments, the calculated  $\epsilon^{15}\text{N}_{\text{NO}_3}$  was -33.1 ‰ ( $R^2 =$   
538 0.86),  $\epsilon^{18}\text{O}_{\text{NO}_3}$  was -10.7 ‰ ( $R^2 = 0.74$ ) and  $\epsilon^{15}\text{N}_{\text{NO}_3}/\epsilon^{18}\text{O}_{\text{NO}_3}$  was 3.1, suggesting  $\delta^{18}\text{O}-$   
539  $\text{NO}_2^-$  equilibration with  $\delta^{18}\text{O}-\text{H}_2\text{O}$  and subsequent  $\text{NO}_2^-$  reoxidation to  $\text{NO}_3^-$ . The isotopic  
540 results for the BioSedGW-Mag/OI/Sd experiments showed a similar trend since  
541 NPDOC released from sediment and groundwater was used as electron donor  
542 (uncomplete denitrification). Calculated  $\epsilon^{15}\text{N}_{\text{NO}_3}$  was -12.0 ‰ ( $R^2 = 0.56$ ),  $\epsilon^{18}\text{O}_{\text{NO}_3}$  was -  
543 10.9 ‰ ( $R^2 = 0.63$ ) and  $\epsilon^{15}\text{N}_{\text{NO}_3}/\epsilon^{18}\text{O}_{\text{NO}_3}$  was 1.1, pointing to a lack of  $\text{NO}_2^-$  reoxidation.

544 In the AbFeNO<sub>2</sub> experiments, the  $\epsilon^{15}\text{N}_{\text{NO}_2}$  ranged from -14.1 ‰ to -17.8 ‰ ( $R^2 > 0.89$ ).  
545 Considering the wide range of  $\epsilon^{15}\text{N}_{\text{NO}_2}$  values reported in the literature, it is not likely  
546 that the  $\text{NO}_2^-$  isotopic characterization can be useful at field-scale to distinguish  
547 homogeneous from heterogeneous reactions or abiotic from microbial  $\text{NO}_2^-$  reduction.  
548 Nevertheless, a high  $\delta^{15}\text{N}-\text{N}_2\text{O}$  enrichment with respect to the substrate could be  
549 indicative of microbial N compounds reduction. Also, modelling the  $\delta^{15}\text{N}-\text{N}_2\text{O}$  by  
550 applying the calculated  $\epsilon^{15}\text{N}_{\text{NO}_3}$  and  $\epsilon^{15}\text{N}_{\text{NO}_2}$  in batch experiments and comparing it with  
551 the determined isotopic composition in the samples can be used to confirm if  $\text{N}_2\text{O}$  is an

1  
2  
3  
4  
5  
6  
7  
8  
9  
10  
11  
12  
13  
14  
15  
16  
17  
18  
19  
20  
21  
22  
23  
24  
25  
26  
27  
28  
29  
30  
31  
32  
33  
34  
35  
36  
37  
38  
39  
40  
41  
42  
43  
44  
45  
46  
47  
48  
49  
50  
51  
52  
53  
54  
55  
56  
57  
58  
59  
60  
61  
62  
63  
64  
65

552 intermediate or final product of the reaction. Therefore,  $\text{NO}_2^-$  abiotic reaction by Fe(II)  
553 oxidation would be advantageous to avoid a water quality decrease due to  $\text{NO}_2^-$   
554 accumulation in denitrification treatments only if the generated  $\text{N}_2\text{O}$  is further reduced  
555 to  $\text{N}_2$  by microorganisms.

556

## 557 **ACKNOWLEDGMENTS**

558 This work has been financed by the following projects: NANOREMOV (CGL2017-  
559 87216-C4-3-R) and ISOTEC (CGL2017-87216-C4-1-R), financed by the Spanish  
560 Government and AEI/FEDER from the UE, and MAG (2017-SGR-1733) from the  
561 Catalan Government. Margalef-Marti, R. is grateful to the Spanish Government for the  
562 Ph.D. grant BES-2015-072882. We would like to thank the CCiT-UB for providing  
563 analytical support, Francesc Roca for his contribution on the Mag nanoparticles  
564 obtainment and Àngels Canals for her contribution on the XRD analysis and results  
565 interpretation.

566

## 567 **REFERENCES**

568 2006/118/EC, 2006. Groundwater Directive. Council Directive 2006/118/EC, of 12  
569 December 2006, on the protection of groundwater against pollution and  
570 deterioration [WWW Document]. Off. J. Eur. Comm. URL  
571 [http://ec.europa.eu/environment/index\\_en.htm](http://ec.europa.eu/environment/index_en.htm) (accessed 4.9.17).

572 91/676/EEC, 1991. Nitrates Directive. Council Directive 91/676/EEC of 12 December  
573 1991, concerning the protection of waters against pollution caused by nitrates  
574 from agricultural sources. [WWW Document]. Off. J. Eur. Comm. URL  
575 [http://ec.europa.eu/environment/index\\_en.htm](http://ec.europa.eu/environment/index_en.htm) (accessed 4.9.17).

576 98/83/EC, 1998. Drinking Water Directive. Council Directive 98/83/EC, of 3 November



1  
2  
3  
4  
5  
6  
7  
8  
9  
10  
11  
12  
13  
14  
15  
16  
17  
18  
19  
20  
21  
22  
23  
24  
25  
26  
27  
28  
29  
30  
31  
32  
33  
34  
35  
36  
37  
38  
39  
40  
41  
42  
43  
44  
45  
46  
47  
48  
49  
50  
51  
52  
53  
54  
55  
56  
57  
58  
59  
60  
61  
62  
63  
64  
65

577 1998, on the quality of water intended for human consumption. [WWW Document].  
578 Off. J. Eur. Comm. URL [http://ec.europa.eu/environment/index\\_en.htm](http://ec.europa.eu/environment/index_en.htm) (accessed  
579 4.9.17).

580 Akunna, J.C., Bizeau, C., Moletta, R., 1993. Nitrate and nitrite reductions with  
581 anaerobic sludge using various carbon sources: Glucose, glycerol, acetic acid,  
582 lactic acid and methanol. *Water Res.* 27, 1303–1312.  
583 [https://doi.org/10.1016/0043-1354\(93\)90217-6](https://doi.org/10.1016/0043-1354(93)90217-6)

584 Aquilina, L., Roques, C., Boisson, A., Vergnaud-Ayraud, V., Labasque, T., Pauwels, H.,  
585 Pételet-Giraud, E., Pettenati, M., Dufresne, A., Bethencourt, L., Bour, O., 2018.  
586 Autotrophic denitrification supported by biotite dissolution in crystalline aquifers  
587 (1): New insights from short-term batch experiments. *Sci. Total Environ.* 619–620,  
588 842–853. <https://doi.org/10.1016/j.scitotenv.2017.11.079>

589 Aravena, R., Robertson, W.D., 1998. Use of multiple isotope tracers to evaluate  
590 denitrification in ground water: study of nitrate from a large-flux septic system  
591 plume. *Ground Water* 36, 975–982.

592 Badr, O., Probert, S.D., 1993. Environmental impacts of atmospheric nitrous oxide.  
593 *Appl. Energy* 44, 197–231. [https://doi.org/10.1016/0306-2619\(93\)90018-K](https://doi.org/10.1016/0306-2619(93)90018-K)

594 Betlach, M.R., Tiedje, J.M., 1981. Kinetic Explanation for Accumulation of Nitrite, Nitric  
595 Oxide, and Nitrous Oxide during Bacterial Denitrification. *Appl. Environ. Microbiol.*  
596 42, 1074–1084. <https://doi.org/Article>

597 Bolleter, W.T., Bushman, C.J., Tidwell, P.W., 1961. Spectrophotometric Determination  
598 of Ammonia as Indophenol. *Anal. Chem.* 33, 592–594.  
599 <https://doi.org/10.1021/ac60172a034>

600 Borden, A.K., Brusseau, M.L., Carroll, K.C., McMillan, A., Akyol, N.H., Berkompas, J.,  
601 Miao, Z., Jordan, F., Tick, G., Waugh, W.J., Glenn, E.P., 2012. Ethanol addition



1  
2  
3  
4  
5  
6  
7  
8  
9  
10  
11  
12  
13  
14  
15  
16  
17  
18  
19  
20  
21  
22  
23  
24  
25  
26  
27  
28  
29  
30  
31  
32  
33  
34  
35  
36  
37  
38  
39  
40  
41  
42  
43  
44  
45  
46  
47  
48  
49  
50  
51  
52  
53  
54  
55  
56  
57  
58  
59  
60  
61  
62  
63  
64  
65

602 for enhancing denitrification at the uranium mill tailing site in Monument Valley,  
603 AZ. *Water, Air, Soil Pollut.* 223, 755–763. [https://doi.org/10.1007/s11270-011-](https://doi.org/10.1007/s11270-011-0899-1)  
604 0899-1

605 Bosch, J., Lee, K.Y., Jordan, G., Kim, K.W., Meckenstock, R.U., 2012. Anaerobic,  
606 nitrate-dependent oxidation of pyrite nanoparticles by *Thiobacillus denitrificans*.  
607 *Environ. Sci. Technol.* 46, 2095–2101. <https://doi.org/10.1021/es2022329>

608 Böttcher, J., Strebel, O., Voerkelius, S., Schmidt, H.-L., 1990. Using isotope  
609 fractionation of nitrate-nitrogen and nitrate-oxygen for evaluation of microbial  
610 denitrification in a sandy aquifer. *J. Hydrol.* 114, 413–424.  
611 [https://doi.org/10.1016/0022-1694\(90\)90068-9](https://doi.org/10.1016/0022-1694(90)90068-9)

612 Braunschweig, J., Bosch, J., Meckenstock, R.U., 2013. Iron oxide nanoparticles in  
613 geomicrobiology: from biogeochemistry to bioremediation. *N. Biotechnol.* 30, 793–  
614 802. <https://doi.org/10.1016/j.nbt.2013.03.008>

615 Bryce, C., Blackwell, N., Schmidt, C., Otte, J., Huang, Y., Kleindienst, S.,  
616 Tomaszewski, E., Schad, M., Warter, V., Peng, C., Byrne, J., Kappler, A., 2018.  
617 Microbial anaerobic Fe(II) oxidation - ecology, mechanisms and environmental  
618 implications. *Environ. Microbiol.* 20, 3462–3483. [https://doi.org/10.1111/1462-](https://doi.org/10.1111/1462-2920.14328)  
619 2920.14328

620 Buchwald, C., Grabb, K., Hansel, C.M., Wankel, S.D., 2016. Constraining the role of  
621 iron in environmental nitrogen transformations: Dual stable isotope systematics of  
622 abiotic NO<sub>2</sub><sup>-</sup> reduction by Fe(II) and its production of N<sub>2</sub>O. *Geochim. Cosmochim.*  
623 *Acta.* <https://doi.org/10.1016/j.gca.2016.04.041>

624 Byrne, J.M., Dopffel, N., Rosso, K.M., Appel, E., 2015. Redox cycling of Fe(II) and  
625 Fe(III) in magnetite by Fe-metabolizing bacteria.  
626 <https://doi.org/10.1126/science.aaa4834>

1  
2  
3  
4  
5  
6  
7  
8  
9  
10  
11  
12  
13  
14  
15  
16  
17  
18  
19  
20  
21  
22  
23  
24  
25  
26  
27  
28  
29  
30  
31  
32  
33  
34  
35  
36  
37  
38  
39  
40  
41  
42  
43  
44  
45  
46  
47  
48  
49  
50  
51  
52  
53  
54  
55  
56  
57  
58  
59  
60  
61  
62  
63  
64  
65

627 Carlson, H.K., Clark, I.C., Blazewicz, S.J., Iavarone, A.T., Coates, J.D., 2013. Fe(II)  
628 oxidation is an innate capability of nitrate-reducing bacteria that involves abiotic  
629 and biotic reactions. *J. Bacteriol.* 195, 3260–3268.  
630 <https://doi.org/10.1128/JB.00058-13>

631 Carrey, R., Otero, N., Vidal-Gavilan, G., Ayora, C., Soler, A., Gómez-Alday, J.J., 2014.  
632 Induced nitrate attenuation by glucose in groundwater: Flow-through experiment.  
633 *Chem. Geol.* 370, 19–28. <https://doi.org/10.1016/j.chemgeo.2014.01.016>

634 Carrey, R., Rodríguez-Escales, P., Soler, A., Otero, N., 2018. Tracing the role of  
635 endogenous carbon in denitrification using wine industry by-product as an external  
636 electron donor: Coupling isotopic tools with mathematical modeling. *J. Environ.*  
637 *Manage.* 207, 105–115. <https://doi.org/10.1016/j.jenvman.2017.10.063>

638 Chen, D., Liu, T., Li, X., Li, F., Luo, X., Wu, Y., Wang, Y., 2018. Biological and chemical  
639 processes of microbially mediated nitrate-reducing Fe(II) oxidation by  
640 *Pseudogulbenkiania* sp. strain 2002. *Chem. Geol.* 476, 59–69.  
641 <https://doi.org/10.1016/j.chemgeo.2017.11.004>

642 Cho, D.W., Song, H., Kim, B., Schwartz, F.W., Jeon, B.H., 2015a. Reduction of nitrate  
643 in groundwater by Fe(0)/Magnetite nanoparticles entrapped in Ca-Alginate beads.  
644 *Water. Air. Soil Pollut.* 226. <https://doi.org/10.1007/s11270-015-2467-6>

645 Cho, D.W., Song, H., Schwartz, F.W., Kim, B., Jeon, B.H., 2015b. The role of  
646 magnetite nanoparticles in the reduction of nitrate in groundwater by zero-valent  
647 iron. *Chemosphere* 125, 41–49.  
648 <https://doi.org/10.1016/j.chemosphere.2015.01.019>

649 Chowdhury, S.R., Yanful, E.K., 2010. Arsenic and chromium removal by mixed  
650 magnetite-maghemite nanoparticles and the effect of phosphate on removal. *J.*  
651 *Environ. Manage.* 91, 2238–2247. <https://doi.org/10.1016/j.jenvman.2010.06.003>

- 1  
2  
3  
4  
5  
6  
7  
8  
9  
10  
11  
12  
13  
14  
15  
16  
17  
18  
19  
20  
21  
22  
23  
24  
25  
26  
27  
28  
29  
30  
31  
32  
33  
34  
35  
36  
37  
38  
39  
40  
41  
42  
43  
44  
45  
46  
47  
48  
49  
50  
51  
52  
53  
54  
55  
56  
57  
58  
59  
60  
61  
62  
63  
64  
65
- 652 Coby, A.J., Picardal, F.W., 2005. Inhibition of  $\text{NO}_3^-$  and  $\text{NO}_2^-$  reduction by microbial  
653 Fe(III) reduction: Evidence of a reaction between  $\text{NO}_2^-$  and cell surface-bound  
654  $\text{Fe}^{2+}$ . *Appl. Environ. Microbiol.* 71, 5267–5274.  
655 <https://doi.org/10.1128/AEM.71.9.5267-5274.2005>
- 656 Cooper, D.C., Picardal, F.W., Schimmelmann, A., Coby, A.J., 2003. Chemical and  
657 Biological Interactions during Nitrate and Goethite Reduction by *Shewanella*  
658 *putrefaciens* 200 Chemical and Biological Interactions during Nitrate and Goethite  
659 Reduction by *Shewanella putrefaciens* 200. *Appl. Environ. Microbiol.* 69, 3517–  
660 3525. <https://doi.org/10.1128/AEM.69.6.3517>
- 661 Coplen, T.B., 2011. Guidelines and recommended terms for expression of stable-  
662 isotope-ratio and gas-ratio measurement results. *Rapid Commun. Mass*  
663 *Spectrom.* 25, 2538–2560. <https://doi.org/10.1002/rcm.5129>
- 664 Crane, R.A., Dickinson, M., Popescu, I.C., Scott, T.B., 2011. Magnetite and zero-valent  
665 iron nanoparticles for the remediation of uranium contaminated environmental  
666 water. *Water Res.* 45, 2931–2942. <https://doi.org/10.1016/j.watres.2011.03.012>
- 667 Devlin, J.F., Eedy, R., Butler, B.J., 2000. The effects of electron donor and granular  
668 iron on nitrate transformation rates in sediments from a municipal water supply  
669 aquifer. *J. Contam. Hydrol.* 46, 81–97. [https://doi.org/10.1016/S0169-7722\(00\)00126-1](https://doi.org/10.1016/S0169-7722(00)00126-1)
- 670  
671 Dhakal, P., Matocha, C.J., Huggins, F.E., Vandiviere, M.M., 2013. Nitrite reactivity with  
672 magnetite. *Environ. Sci. Technol.* 47, 6206–6213.  
673 <https://doi.org/10.1021/es304011w>
- 674 Fukada, T., Hiscock, K.M., Dennis, P.F., Grischek, T., 2003. A dual isotope approach  
675 to identify denitrification in groundwater at a river-bank infiltration site. *Water Res.*  
676 37, 3070–3078. [https://doi.org/10.1016/S0043-1354\(03\)00176-3](https://doi.org/10.1016/S0043-1354(03)00176-3)

1  
2  
3  
4  
5  
6  
7  
8  
9  
10  
11  
12  
13  
14  
15  
16  
17  
18  
19  
20  
21  
22  
23  
24  
25  
26  
27  
28  
29  
30  
31  
32  
33  
34  
35  
36  
37  
38  
39  
40  
41  
42  
43  
44  
45  
46  
47  
48  
49  
50  
51  
52  
53  
54  
55  
56  
57  
58  
59  
60  
61  
62  
63  
64  
65

677 Ge, S., Peng, Y., Wang, S., Lu, C., Cao, X., Zhu, Y., 2012. Nitrite accumulation under  
678 constant temperature in anoxic denitrification process: The effects of carbon  
679 sources and COD/NO<sub>3</sub>-N. *Bioresour. Technol.* 114, 137–143.  
680 <https://doi.org/10.1016/j.biortech.2012.03.016>

681 Gibert, O., Pomierny, S., Rowe, I., Kalin, R.M., 2008. Selection of organic substrates as  
682 potential reactive materials for use in a denitrification permeable reactive barrier  
683 (PRB). *Bioresour. Technol.* 99, 7587–7596.  
684 <https://doi.org/10.1016/j.biortech.2008.02.012>

685 Gorski, C. a, Nurmi, J.T., Tratnyek, P.G., Hofstetter, T.B., Scherer, M.M., 2010. Redox  
686 Behavior of Magnetite: Reduction. *Environ. Sci. Technol.* 44, 55–60.  
687 <https://doi.org/10.1021/es9016848>

688 Grabb, K.C., Buchwald, C., Hansel, C.M., Wankel, S.D., 2017. A dual nitrite isotopic  
689 investigation of chemodenitrification by mineral-associated Fe(II) and its  
690 production of nitrous oxide. *Geochim. Cosmochim. Acta* 196, 388–402.  
691 <https://doi.org/10.1016/j.gca.2016.10.026>

692 Granger, J., Sigman, D.M., Lehmann, M.F., Tortell, P.D., 2008. Nitrogen and oxygen  
693 isotope fractionation during dissimilatory nitrate reduction by denitrifying bacteria.  
694 *Limnol. Oceanogr.* 53, 2533–2545. <https://doi.org/10.4319/lo.2008.53.6.2533>

695 Grau-Martínez, A., Torrentó, C., Carrey, R., Rodríguez-Escales, P., Domènech, C.,  
696 Ghiglieri, G., Soler, A., Otero, N., 2017. Feasibility of two low-cost organic  
697 substrates for inducing denitrification in artificial recharge ponds: Batch and flow-  
698 through experiments. *J. Contam. Hydrol.* 198, 48–58.  
699 <https://doi.org/10.1016/j.jconhyd.2017.01.001>

700 He, S., Tominski, C., Kappler, A., Behrens, S., Roden, E.E., 2016. Metagenomic  
701 analyses of the autotrophic Fe(II)-oxidizing, nitrate-reducing enrichment culture

1  
2  
3  
4  
5 702 KS. Appl. Environ. Microbiol. 82, 2656–2668. <https://doi.org/10.1128/AEM.03493->  
6  
7 703 15  
8  
9  
10 704 He, Y., Lin, H., Dong, Y., Li, B., Wang, L., Chu, S., Luo, M., Liu, J., 2018. Zeolite  
11 supported Fe/Ni bimetallic nanoparticles for simultaneous removal of nitrate and  
12 phosphate: Synergistic effect and mechanism. Chem. Eng. J. 347, 669–681.  
13 <https://doi.org/10.1016/j.cej.2018.04.088>  
14  
15 708 Heil, J., Wolf, B., Brüggemann, N., Emmenegger, L., Tuzson, B., Vereecken, H., Mohn,  
16 J., 2014. Site-specific <sup>15</sup>N isotopic signatures of abiotically produced N<sub>2</sub>O.  
17 Geochim. Cosmochim. Acta 139, 72–82. <https://doi.org/10.1016/j.gca.2014.04.037>  
18  
19 710  
20  
21  
22 711 Hernández-del Amo, E., Menció, A., Gich, F., Mas-Pla, J., Bañeras, L., 2018. Isotope  
23 and microbiome data provide complementary information to identify natural nitrate  
24 attenuation processes in groundwater. Sci. Total Environ. 613–614, 579–591.  
25 <https://doi.org/10.1016/j.scitotenv.2017.09.018>  
26  
27 712  
28  
29 713  
30  
31  
32 715 Jamieson, J., Prommer, H., Kaksonen, A.H., Sun, J., Siade, A.J., Yusov, A., Bostick,  
33 B., 2018. Identifying and Quantifying the Intermediate Processes during Nitrate-  
34 Dependent Iron(II) Oxidation. Environ. Sci. Technol. 52, 5771–5781.  
35 <https://doi.org/10.1021/acs.est.8b01122>  
36  
37 716  
38  
39 717  
40  
41  
42 719 Jones, L.C., Peters, B., Lezama Pacheco, J.S., Casciotti, K.L., Fendorf, S., 2015.  
43 Stable Isotopes and Iron Oxide Mineral Products as Markers of  
44 Chemodenitrification. Environ. Sci. Technol. 49, 3444–3452.  
45 <https://doi.org/10.1021/es504862x>  
46  
47 720  
48  
49 721  
50  
51  
52 723 Jurado, A., Borges, A. V., Brouyère, S., 2017. Dynamics and emissions of N<sub>2</sub>O in  
53 groundwater: A review. Sci. Total Environ. 584–585, 207–218.  
54 <https://doi.org/10.1016/j.scitotenv.2017.01.127>  
55  
56 724  
57  
58 725  
59  
60 726 Kampschreur, M.J., Kleerebezem, R., de Vet, W.W.J.M., Van Loosdrecht, M.C.M.,  
61  
62  
63  
64  
65

- 1  
2  
3  
4  
5  
6  
7  
8  
9  
10  
11  
12  
13  
14  
15  
16  
17  
18  
19  
20  
21  
22  
23  
24  
25  
26  
27  
28  
29  
30  
31  
32  
33  
34  
35  
36  
37  
38  
39  
40  
41  
42  
43  
44  
45  
46  
47  
48  
49  
50  
51  
52  
53  
54  
55  
56  
57  
58  
59  
60  
61  
62  
63  
64  
65
- 727 2011. Reduced iron induced nitric oxide and nitrous oxide emission. *Water Res.*  
728 45, 5945–5952. <https://doi.org/10.1016/j.watres.2011.08.056>
- 729 Klueglein, N., Kappler, A., 2013. Abiotic oxidation of Fe(II) by reactive nitrogen species  
730 in cultures of the nitrate-reducing Fe(II) oxidizer *Acidovorax* sp. BoFeN1 -  
731 questioning the existence of enzymatic Fe(II) oxidation. *Geobiology* 11, 180–190.  
732 <https://doi.org/10.1111/gbi.12019>
- 733 Knöller, K., Vogt, C., Haupt, M., Feisthauer, S., Richnow, H.H., 2011. Experimental  
734 investigation of nitrogen and oxygen isotope fractionation in nitrate and nitrite  
735 during denitrification. *Biogeochemistry* 103, 371–384.  
736 <https://doi.org/10.1007/s10533-010-9483-9>
- 737 Knowles, R., 1982. Denitrification. *Microbiol. Rev.* 46, 43–70.
- 738 Koch, H., Lücker, S., Albertsen, M., Kitzinger, K., Herbold, C., Spieck, E., 2015.  
739 Expanded metabolic versatility of ubiquitous nitrite-oxidizing bacteria from the  
740 genus *Nitrospira* 112, 11371–11376. <https://doi.org/10.1073/pnas.1506533112>
- 741 Liu, T., Chen, D., Luo, X., Li, X., Li, F., 2018. Microbially mediated nitrate-reducing  
742 Fe(II) oxidation: Quantification of chemodenitrification and biological reactions.  
743 *Geochim. Cosmochim. Acta.* <https://doi.org/10.1016/j.gca.2018.06.040>
- 744 Margalef-Marti, R., Carrey, R., Merchán, D., Soler, A., Causapé, J., Otero, N., 2019a.  
745 Feasibility of using rural waste products to increase the denitrification efficiency in  
746 a surface flow constructed wetland. *J. Hydrol.* 124035.  
747 <https://doi.org/10.1016/j.jhydrol.2019.124035>
- 748 Margalef-Marti, R., Carrey, R., Soler, A., Otero, N., 2019b. Evaluating the potential use  
749 of a dairy industry residue to induce denitri fi cation in polluted water bodies : A fl  
750 ow-through experiment. *J. Environ. Manage.* 245, 86–94.  
751 <https://doi.org/10.1016/j.jenvman.2019.03.086>

1  
2  
3  
4  
5  
6  
7  
8  
9  
10  
11  
12  
13  
14  
15  
16  
17  
18  
19  
20  
21  
22  
23  
24  
25  
26  
27  
28  
29  
30  
31  
32  
33  
34  
35  
36  
37  
38  
39  
40  
41  
42  
43  
44  
45  
46  
47  
48  
49  
50  
51  
52  
53  
54  
55  
56  
57  
58  
59  
60  
61  
62  
63  
64  
65

752 Margalef-Marti, R., Carrey, R., Viladés, M., Jubany, I., Vilanova, E., Grau, R., Soler, A.,  
753 Otero, N., 2019c. Use of nitrogen and oxygen isotopes of dissolved nitrate to trace  
754 field-scale induced denitrification efficiency throughout an in-situ groundwater  
755 remediation strategy. *Sci. Total Environ.*  
756 <https://doi.org/10.1016/j.scitotenv.2019.06.003>

757 Mariotti, A., Germon, J.C., Hubert, P., Kaiser, P., Letolle, R., Tardieux, A., Tardieux, P.,  
758 1981. Experimental determination of nitrogen kinetic isotope fractionation: Some  
759 principles; illustration for the denitrification and nitrification processes. *Plant Soil*  
760 62, 413–430. <https://doi.org/10.1007/BF02374138>

761 Mariotti, A., Landreau, A., Simon, B., 1988. <sup>15</sup>N isotope biogeochemistry and natural  
762 denitrification process in groundwater: Application to the chalk aquifer of northern  
763 France. *Geochim. Cosmochim. Acta* 52, 1869–1878. [https://doi.org/10.1016/0016-](https://doi.org/10.1016/0016-7037(88)90010-5)  
764 [7037\(88\)90010-5](https://doi.org/10.1016/0016-7037(88)90010-5)

765 Martin, T.S., Casciotti, K.L., 2016. Nitrogen and oxygen isotopic fractionation during  
766 microbial nitrite reduction. *Limnol. Oceanogr.* 61, 1134-1143. [https://doi.org/](https://doi.org/10.1002/lno.10278)  
767 [10.1002/lno.10278](https://doi.org/10.1002/lno.10278)

768 Matocha, C.J., Coyne, M.S., 2007. Short-term Response of Soil Iron to Nitrate Addition.  
769 *Soil Sci. Soc. Am. J.* 71, 108. <https://doi.org/10.2136/sssaj2005.0170>

770 McIlvin, M.R., Altabet, M.A., 2005. Chemical conversion of nitrate and nitrite to nitrous  
771 oxide for nitrogen and oxygen isotopic analysis in freshwater and seawater. *Anal*  
772 *Chem* 77, 5589–5595. <https://doi.org/10.1021/ac050528s>

773 Meckenstock, R.U., Morasch, B., Griebler, C., Richnow, H.H., 2004. Stable isotope  
774 fractionation analysis as a tool to monitor biodegradation in contaminated  
775 aquifers. *J. Contam. Hydrol.* 75, 215–255.  
776 <https://doi.org/10.1016/j.jconhyd.2004.06.003>

1  
2  
3  
4  
5  
6  
7  
8  
9  
10  
11  
12  
13  
14  
15  
16  
17  
18  
19  
20  
21  
22  
23  
24  
25  
26  
27  
28  
29  
30  
31  
32  
33  
34  
35  
36  
37  
38  
39  
40  
41  
42  
43  
44  
45  
46  
47  
48  
49  
50  
51  
52  
53  
54  
55  
56  
57  
58  
59  
60  
61  
62  
63  
64  
65

777 Melton, E.D., Swanner, E.D., Behrens, S., Schmidt, C., Kappler, A., 2014. The interplay  
778 of microbially mediated and abiotic reactions in the biogeochemical Fe cycle. *Nat.*  
779 *Rev. Microbiol.* 12, 797–808. <https://doi.org/10.1038/nrmicro3347>

780 Morley, N., Baggs, E.M., Dörsch, P., Bakken, L., 2008. Production of NO, N<sub>2</sub>O and N<sub>2</sub>  
781 by extracted soil bacteria, regulation by NO<sub>2</sub><sup>-</sup> and O<sub>2</sub> concentrations. *FEMS*  
782 *Microbiol. Ecol.* 65, 102–112. <https://doi.org/10.1111/j.1574-6941.2008.00495.x>

783 Otero, N., Torrentó, C., Soler, A., Menció, A., Mas-Pla, J., 2009. Monitoring  
784 groundwater nitrate attenuation in a regional system coupling hydrogeology with  
785 multi-isotopic methods: The case of Plana de Vic (Osona, Spain). *Agric. Ecosyst.*  
786 *Environ.* 133, 103–113. <https://doi.org/10.1016/j.agee.2009.05.007>

787 Pantke, C., Obst, M., Benzerara, K., Morin, G., Ona-nguema, G., Dippon, U., Kappler,  
788 A., 2012. Green Rust Formation during Fe(II) Oxidation by the Nitrate-Reducing  
789 *Acidovorax* sp. Strain BoFeN1. *Environ. Sci. Technol.* 1439–1446.  
790 <https://doi.org/10.1021/es2016457>

791 Price, A., Pearson, V.K., Schwenzer, S.P., Miot, J., Olsson-Francis, K., 2018. Nitrate-  
792 dependent iron oxidation: A potential Mars metabolism. *Front. Microbiol.* 9, 1–15.  
793 <https://doi.org/10.3389/fmicb.2018.00513>

794 Rakshit, S., Matocha, C.J., Coyne, M.S., Sarkar, D., 2016. Nitrite reduction by Fe(II)  
795 associated with kaolinite. *Int. J. Environ. Sci. Technol.* 13, 1329–1334.  
796 <https://doi.org/10.1007/s13762-016-0971-x>

797 Reay, D.S., Davidson, E.A., Smith, K.A., Smith, P., Melillo, J.M., Dentener, F., Crutzen,  
798 P.J., 2012. Global agriculture and nitrous oxide emissions. *Nat. Clim. Chang.* 2,  
799 410–416. <https://doi.org/10.1038/nclimate1458>

800 Rivett, M.O., Buss, S.R., Morgan, P., Smith, J.W.N., Bemment, C.D., 2008. Nitrate  
801 attenuation in groundwater: A review of biogeochemical controlling processes.



1  
2  
3  
4  
5  
6  
7  
8  
9  
10  
11  
12  
13  
14  
15  
16  
17  
18  
19  
20  
21  
22  
23  
24  
25  
26  
27  
28  
29  
30  
31  
32  
33  
34  
35  
36  
37  
38  
39  
40  
41  
42  
43  
44  
45  
46  
47  
48  
49  
50  
51  
52  
53  
54  
55  
56  
57  
58  
59  
60  
61  
62  
63  
64  
65

802 Water Res. 42, 4215–4232. <https://doi.org/10.1016/j.watres.2008.07.020>

803 Ryabenko, E., Altabet, M. a., Wallace, D.W.R., 2009. Effect of chloride on the chemical  
804 conversion of nitrate to nitrous oxide for  $\delta^{15}\text{N}$  analysis. Limnol. Oceanogr. Methods  
805 7, 545–552. <https://doi.org/10.4319/lom.2009.7.545>

806 Si, Z., Song, X., Wang, Y., Cao, X., Zhao, Y., Wang, B., Chen, Y., Arefe, A., 2018.  
807 Intensified heterotrophic denitrification in constructed wetlands using four solid  
808 carbon sources: Denitrification efficiency and bacterial community structure.  
809 Bioresour. Technol. 267, 416–425. <https://doi.org/10.1016/j.biortech.2018.07.029>

810 Smith, R.L., Kent, D.B., Repert, D.A., Böhlke, J.K., 2017. Anoxic nitrate reduction  
811 coupled with iron oxidation and attenuation of dissolved arsenic and phosphate in  
812 a sand and gravel aquifer. Geochim. Cosmochim. Acta 196, 102–120.  
813 <https://doi.org/10.1016/j.gca.2016.09.025>

814 Smith, R.L., Miller, D.N., Brooks, M.H., Widdowson, M.A., Killingstad, M.W., 2001. In  
815 situ stimulation of groundwater denitrification with formate to remediate nitrate  
816 contamination. Environ. Sci. Technol. 35, 196–203.  
817 <https://doi.org/10.1021/es001360p>

818 Straub, K.L., Benz, M., Schink, B., Widdel, F., 1996. Anaerobic, nitrate-dependent  
819 microbial oxidation of ferrous iron. Appl. Environ. Microbiol. 62, 1458–1460.  
820 <https://doi.org/10.1016/j.watres.2008.10.055>

821 Tai, Y.L., Dempsey, B.A., 2009. Nitrite reduction with hydrous ferric oxide and Fe(II):  
822 Stoichiometry, rate, and mechanism. Water Res. 43, 546–552.  
823 <https://doi.org/10.1016/j.watres.2008.10.055>

824 Torrentó, C., Cama, J., Urmeneta, J., Otero, N., Soler, A., 2010. Denitrification of  
825 groundwater with pyrite and *Thiobacillus denitrificans*. Chem. Geol. 278, 80–91.  
826 <https://doi.org/10.1016/j.chemgeo.2010.09.003>

1  
2  
3  
4  
5  
6  
7  
8  
9  
10  
11  
12  
13  
14  
15  
16  
17  
18  
19  
20  
21  
22  
23  
24  
25  
26  
27  
28  
29  
30  
31  
32  
33  
34  
35  
36  
37  
38  
39  
40  
41  
42  
43  
44  
45  
46  
47  
48  
49  
50  
51  
52  
53  
54  
55  
56  
57  
58  
59  
60  
61  
62  
63  
64  
65

827 Torrentó, C., Urmeneta, J., Otero, N., Soler, A., Viñas, M., Cama, J., 2011. Enhanced  
828 denitrification in groundwater and sediments from a nitrate-contaminated aquifer  
829 after addition of pyrite. *Chem. Geol.* 287, 90–101.  
830 <https://doi.org/10.1016/j.chemgeo.2011.06.002>

831 Trois, C., Pisano, G., Oxarango, L., 2010. Alternative solutions for the bio-denitrification  
832 of landfill leachates using pine bark and compost. *J. Hazard. Mater.* 178, 1100–  
833 1105. <https://doi.org/10.1016/j.jhazmat.2010.01.054>

834 Tsushima, K., Ueda, S., Ohno, H., Ogura, N., Katase, T., Watanabe, K., 2006. Nitrate  
835 decrease with isotopic fractionation in riverside sediment column during infiltration  
836 experiment. *Water. Air. Soil Pollut.* 174, 47–61. [https://doi.org/10.1007/s11270-](https://doi.org/10.1007/s11270-005-9024-7)  
837 [005-9024-7](https://doi.org/10.1007/s11270-005-9024-7)

838 Vidal-Gavilan, G., Folch, A., Otero, N., Solanas, A.M., Soler, A., 2013. Isotope  
839 characterization of an in situ biodenitrification pilot-test in a fractured aquifer. *Appl.*  
840 *Geochemistry* 32, 153–163. <https://doi.org/10.1016/j.apgeochem.2012.10.033>

841 Vitòria, L., Soler, A., Canals, À., Otero, N., 2008. Environmental isotopes (N, S, C, O,  
842 D) to determine natural attenuation processes in nitrate contaminated waters:  
843 Example of Osona (NE Spain). *Appl. Geochemistry* 23, 3597–3611.  
844 <https://doi.org/10.1016/j.apgeochem.2008.07.018>

845 Vitousek, P.M., Aber, J.D., Howarth, R.W., Likens, G.E., Matson, P.A., Schindler, D.W.,  
846 Schlesinger, W.H., Tilman, D.G., 1997. Summary for Policymakers, in:  
847 Intergovernmental Panel on Climate Change (Ed.), *Climate Change 2013 - The*  
848 *Physical Science Basis*. Cambridge University Press, Cambridge, pp. 1–30.  
849 <https://doi.org/10.1017/CBO9781107415324.004>

850 Wang, M., Hu, R., Zhao, J., Kuzyakov, Y., Liu, S., 2016. Iron oxidation affects nitrous  
851 oxide emissions via donating electrons to denitrification in paddy soils. *Geoderma*

1  
2  
3  
4  
5  
6  
7  
8  
9  
10  
11  
12  
13  
14  
15  
16  
17  
18  
19  
20  
21  
22  
23  
24  
25  
26  
27  
28  
29  
30  
31  
32  
33  
34  
35  
36  
37  
38  
39  
40  
41  
42  
43  
44  
45  
46  
47  
48  
49  
50  
51  
52  
53  
54  
55  
56  
57  
58  
59  
60  
61  
62  
63  
64  
65

852 271, 173–180. <https://doi.org/10.1016/j.geoderma.2016.02.022>

853 Ward, M.H., DeKok, T.M., Levallois, P., Brender, J., Gulis, G., Nolan, B.T.,  
854 VanDerslice, J., 2005. Workgroup Report: Drinking-Water Nitrate and Health—  
855 Recent Findings and Research Needs. *Environ. Health Perspect.* 113, 1607–  
856 1614. <https://doi.org/10.1289/ehp.8043>

857 Weber, K.A., Achenbach, L.A., Coates, J.D., 2006. Microorganisms pumping iron:  
858 Anaerobic microbial iron oxidation and reduction. *Nat. Rev. Microbiol.* 4, 752–764.  
859 <https://doi.org/10.1038/nrmicro1490>

860 Weymann, D., Geistlinger, H., Well, R., Von Der Heide, C., Flessa, H., 2010. Kinetics  
861 of N<sub>2</sub>O production and reduction in a nitrate-contaminated aquifer inferred from  
862 laboratory incubation experiments. *Biogeosciences* 7, 1953–1972.  
863 <https://doi.org/10.5194/bg-7-1953-2010>

864 Wunderlich, A., Meckenstock, R., Einsiedl, F., 2012. Effect of different carbon  
865 substrates on nitrate stable isotope fractionation during microbial denitrification.  
866 *Environ. Sci. Technol.* 46, 4861–4868. <https://doi.org/10.1021/es204075b>

867 Yan, R., Kappler, A., Muehe, E.M., Knorr, K.H., Horn, M.A., Poser, A., Lohmayer, R.,  
868 Peiffer, S., 2019. Effect of Reduced Sulfur Species on Chemolithoautotrophic  
869 Pyrite Oxidation with Nitrate. *Geomicrobiol. J.*  
870 <https://doi.org/10.1080/01490451.2018.1489915>

871 Yang, Y., Chen, T., Morrison, L., Gerrity, S., Collins, G., Porca, E., Li, R., Zhan, X.,  
872 2017. Nanostructured pyrrhotite supports autotrophic denitrification for  
873 simultaneous nitrogen and phosphorus removal from secondary effluents. *Chem.*  
874 *Eng. J.* 328, 511–518. <https://doi.org/10.1016/j.cej.2017.07.061>

875 Zelmanov, G., Semiat, R., 2008. Iron(3) oxide-based nanoparticles as catalysts in  
876 advanced organic aqueous oxidation. *Water Res.* 42, 492–498.

1  
2  
3  
4  
5  
6  
7  
8  
9  
10  
11  
12  
13  
14  
15  
16  
17  
18  
19  
20  
21  
22  
23  
24  
25  
26  
27  
28  
29  
30  
31  
32  
33  
34  
35  
36  
37  
38  
39  
40  
41  
42  
43  
44  
45  
46  
47  
48  
49  
50  
51  
52  
53  
54  
55  
56  
57  
58  
59  
60  
61  
62  
63  
64  
65

877 <https://doi.org/10.1016/j.watres.2007.07.045>

878 Zhou, J., Wang, H., Yang, K., Ji, B., Chen, D., Zhang, H., Sun, Y., Tian, J., 2016.  
879 Autotrophic denitrification by nitrate-dependent Fe(II) oxidation in a continuous up-  
880 flow biofilter. *Bioprocess Biosyst. Eng.* 39, 277–284.  
881 <https://doi.org/10.1007/s00449-015-1511-7>

882 Zumft, W.G., 1997. Cell biology and molecular basis of denitrification. *Microbiol. Mol.*  
883 *Biol. Rev.* 61, 533–616.

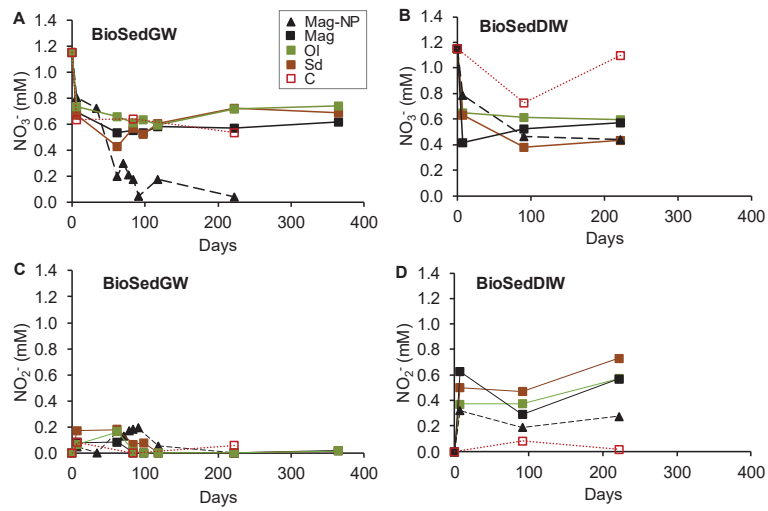


**Figure 1.  $\text{NO}_3^-$  reduction in microbial experiments.**  $\text{NO}_3^-$  (A, B) and  $\text{NO}_2^-$  (C, D) concentrations measured in the BioSedGW (A, C) and BioSedDIW (B, D) experiments, containing groundwater or deionized water, respectively. Both types of experiments contained sediment. In experiments labelled as Mag-NP, Mag, Sd, Ol minerals were added while in experiments labelled as C (control) no minerals were added.

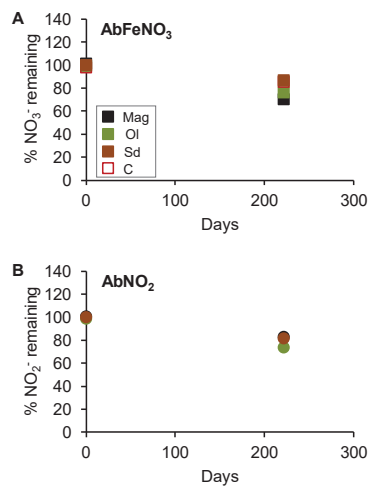


**Figure 2. Lack of abiotic reactivity between NO<sub>3</sub><sup>-</sup> and Fe(II) (dissolved or mineral) and between NO<sub>2</sub><sup>-</sup> and the micro-sized minerals.** Remaining NO<sub>3</sub><sup>-</sup> (squares) or NO<sub>2</sub><sup>-</sup> (circles) concentration in the AbFeNO<sub>3</sub> (A) and AbNO<sub>2</sub> (B) experiments, that contained deionized water with NO<sub>3</sub><sup>-</sup> or NO<sub>2</sub><sup>-</sup>, respectively. In experiments labelled as Mag-NP, Mag, Sd, Ol minerals were added while in experiments labelled as C (control) no minerals were added. Dissolved Fe<sup>2+</sup> was added in the AbFeNO<sub>3</sub> experiments.

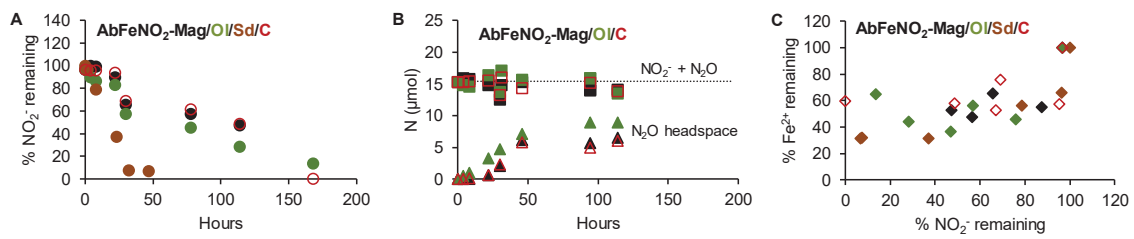


**Figure 3. Abiotic reactivity between  $\text{NO}_2^-$  and dissolved  $\text{Fe}^{2+}$ .** For the AbFeNO<sub>2</sub> experiments, (A) show the remaining  $\text{NO}_2^-$ . In (B), the accumulated  $\text{N}_2\text{O}$  is presented as triangles, the sum of accumulated  $\text{N}_2\text{O}$  and remaining  $\text{NO}_2^-$  is presented as squares and the dotted line reflects the  $\text{NO}_2^-$  initial content. (C) show the remaining dissolved  $\text{Fe}^{2+}$ . These experiments contained synthetic water with  $\text{NO}_2^-$  and dissolved  $\text{Fe}^{2+}$ . In experiments labelled as Mag, Sd or OI, minerals were added while in experiments labelled as C (control), no minerals were added.

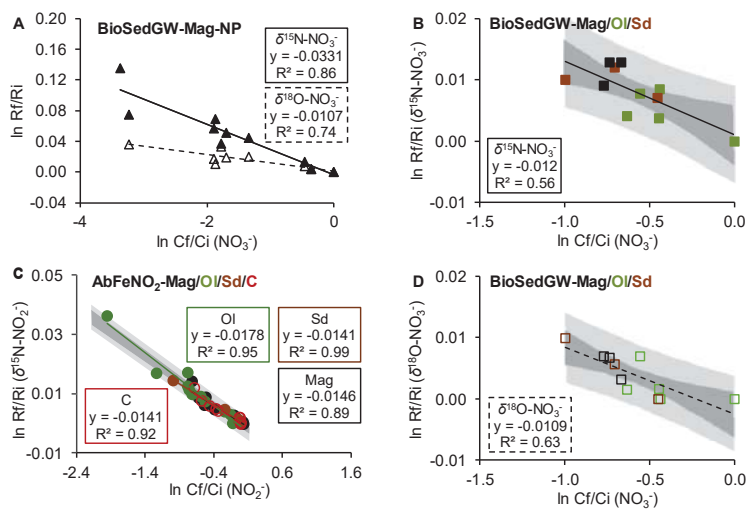


**Figure 4.  $\text{NO}_3^-$  and  $\text{NO}_2^-$   $\epsilon$  calculation.** (A, B, D) show the fractionation for the  $\delta^{15}\text{N-NO}_3^-$  (continuous line) and  $\delta^{18}\text{O-NO}_3^-$  (dotted line) in the microbial tests (BioSedGW-Mag-NP and BioSedGW-Mag/OI/Sd/C, respectively). These experiments contained  $\text{NO}_3^-$  polluted groundwater and sediment plus minerals (Mag-NP, Mag, OI, Sd). (C) show the  $\delta^{15}\text{N-NO}_2^-$  fractionation in the abiotic tests (AbFe $\text{NO}_2$ ) containing synthetic water with  $\text{NO}_2^-$  and dissolved  $\text{Fe}^{2+}$  and involving the addition or lack of micro-sized minerals (Mag, OI, Sd or C (control)). In the plots including different experiments, the shaded areas reflect the 95 % confidence interval.



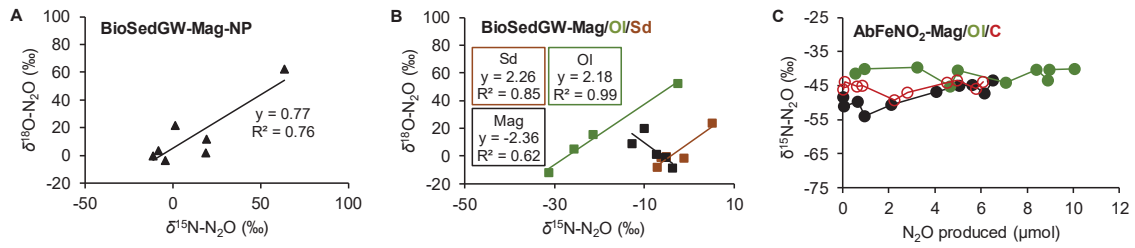


**Figure 5. N<sub>2</sub>O isotopic composition.**  $\delta^{15}\text{N-N}_2\text{O}$  versus  $\delta^{18}\text{O-N}_2\text{O}$  plots for the microbial experiments BioSedGW-Mag-NP (**A**) and BioSedGW-Mag/OI/Sd (**B**), which contained NO<sub>3</sub><sup>-</sup> polluted groundwater and sediment plus minerals (Mag-NP or micro-sized Mag, OI, Sd). For the abiotic tests (AbFeNO<sub>2</sub>), which contained deionized water with NO<sub>2</sub><sup>-</sup> and dissolved Fe<sup>2+</sup> with or without addition of minerals (Mag, OI or C (control)), the  $\delta^{15}\text{N-N}_2\text{O}$  evolution along N<sub>2</sub>O production is shown (**C**).

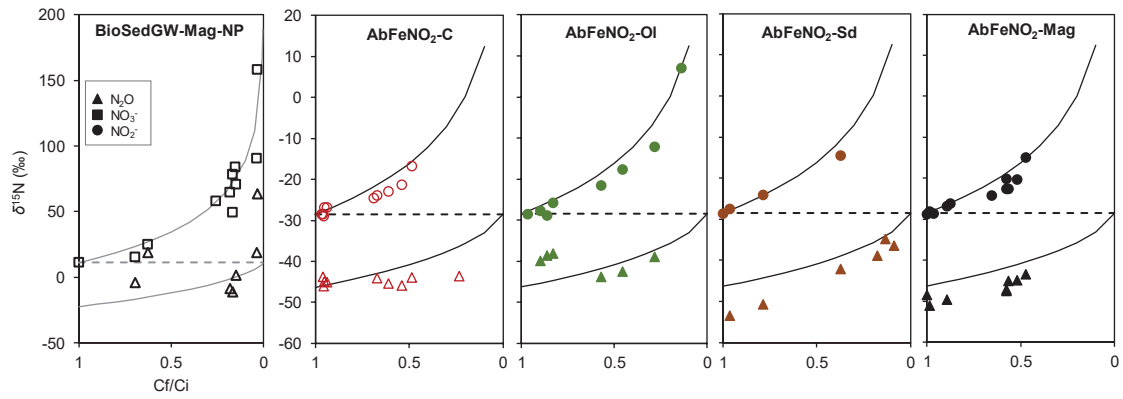


**Figure 6. Modelled and measured  $\delta^{15}\text{N}$  of the remaining substrate and generated  $\text{N}_2\text{O}$ .** The BioSedGW-Mag-NP microcosms contained  $\text{NO}_3^-$  polluted groundwater and sediment plus Mag-NP (microbial). The AbFeNO<sub>2</sub> tests contained deionized water with  $\text{NO}_2^-$  and dissolved  $\text{Fe}^{2+}$  and involved the addition or lack of micro-sized minerals (Mag, Sd, OI or C (control)) (abiotic). This model was first described by Mariotti et al. (1981) and was drawn using the  $\epsilon$  values determined for the experiments.

**Table 1. Microbial and abiotic experiments.** Content of the batch experiments. N stands for the number of identical bottles. DIW refers to deionized water. (\*) The number of bottles is for each mineral (Min) used (Mag, Ol, Sd, Mag-NP). C refers to the control without mineral.

Experiment	Conditions	N	Code
Microbial NO <sub>3</sub> <sup>-</sup> reduction (groundwater)	Sediment (2.5 g) + groundwater (15 mL, 1 mM NO <sub>3</sub> <sup>-</sup> )	3	BioSedGW-C
	Sediment (2.5 g) + groundwater (15 mL, 1 mM NO <sub>3</sub> <sup>-</sup> ) + mineral (100 mg)	8 (*)	BioSedGW-Min
Microbial NO <sub>3</sub> <sup>-</sup> reduction (DIW)	Sediment (2.5 g) + DIW (15 mL, 1 mM NO <sub>3</sub> <sup>-</sup> )	3	BioSedDIW-C
	Sediment (2.5 g) + DIW (15 mL, 1 mM NO <sub>3</sub> <sup>-</sup> ) + mineral (100 mg)	3 (*)	BioSedDIW-Min
Blank	Sediment (2.5 g) + MilliQ water (15 mL)	3	Blank
Abiotic NO <sub>3</sub> <sup>-</sup> reduction (synthetic water + Fe <sup>2+</sup> )	Synthetic water (10 mL, 1 mM NO <sub>3</sub> <sup>-</sup> ) + FeCl <sub>2</sub> (5 mM)	3	AbFeNO <sub>3</sub> -C
	Synthetic water (10 mL, 1 mM NO <sub>3</sub> <sup>-</sup> ) + FeCl <sub>2</sub> (5 mM) + mineral (50 mg)	3 (*)	AbFeNO <sub>3</sub> -Min
Abiotic NO <sub>2</sub> <sup>-</sup> reduction (synthetic water)	Synthetic water (10 mL, 1 mM NO <sub>2</sub> <sup>-</sup> ) + mineral (50 mg)	3 (*)	AbNO <sub>2</sub> -Min
Abiotic NO <sub>2</sub> <sup>-</sup> reduction (synthetic water + Fe <sup>2+</sup> )	Synthetic water (10 mL, 1 mM NO <sub>2</sub> <sup>-</sup> ) + FeCl <sub>2</sub> (5 mM)	8	AbFeNO <sub>2</sub> -C
	Synthetic water (10 mL, 1 mM NO <sub>2</sub> <sup>-</sup> ) + FeCl <sub>2</sub> (5 mM) + mineral (50 mg)	8 (*)	AbFeNO <sub>2</sub> -Min

**Table 2. Range of  $\epsilon^{15}\text{N}$ ,  $\epsilon^{18}\text{O}$  and  $\epsilon^{15}\text{N}/\epsilon^{18}\text{O}$  values reported in the literature for  $\text{NO}_3^-$  and  $\text{NO}_2^-$  reduction laboratory experiments.** Both the microbial and abiotic reductions are included. For pure culture experiments, the enzymes are specified inside parentheses (if reported). n.d. = no determined.

ELECTRON ACCEPTOR	ELECTRON DONOR	INVOLVED MICROORGANISMS	$\epsilon^{15}\text{N}$	$\epsilon^{18}\text{O}$	$\epsilon^{15}\text{N}/\epsilon^{18}\text{O}$	REFERENCE
$\text{NO}_3^-$	$\text{C}_{\text{org}}$	<i>Ochrobactrum</i> sp., <i>Paracoccus denitrificans</i> , <i>Pseudomonas stutzeri</i> (NAR)	-5.4 to -26.6	-4.8 to -22.8	1.0 to 1.2	(Granger et al., 2008)
$\text{NO}_3^-$	$\text{C}_{\text{org}}$	<i>Rhodobacter sphaeroides</i> (NAP)	-16	-8.9	1.8	
$\text{NO}_3^-$	$\text{C}_{\text{org}}$	<i>Pseudomonas pseudobalcaligenes</i> , <i>Azoarcus</i> sp.	-8.6 to -16.2	-4.0 to -7.3	1.3 to 3.0	(Knöller et al., 2011)
$\text{NO}_3^-$	$\text{C}_{\text{org}}$	<i>Thauera aromatica</i> , <i>Aromatoleum aromaticum</i>	-17.3 to -23.5	-15.9 to -23.7	1.0 to 1.2	(Wunderlich et al., 2012)
$\text{NO}_3^-$	Compounds from riparian sediments and groundwater	Microorganisms from riparian sediments and groundwater	-32.9 to -34.1	n.d.	n.d.	(Tsushima et al., 2006)
$\text{NO}_3^-$	Pyrite	<i>Thiobacillus denitrificans</i>	-15.0 to -27.6	-13.5 to -21.3	1.1 to 1.3	(Torrentó et al., 2011, 2010)
$\text{NO}_2^-$	$\text{C}_{\text{org}}$	<i>Pseudomonas aeruginosa</i> , <i>Pseudomonas chloraphis</i> , <i>Pseudomonas stutzeri</i> (Fe-NIR)	-3 to -11	-2 to -12	0.7 to 3.3	(Martin and Casciotti, 2016)
$\text{NO}_2^-$	$\text{C}_{\text{org}}$	<i>Achromobacter xylosoxidans</i> , <i>Ochrobactrum</i> sp., <i>Pseudomonas aureofaciens</i> (Cu-NIR)	-19 to -26	0 to -6	3.1 to 22.0	
$\text{NO}_2^-$	Nontronite	Abiotic	-11.1	-10.4	1.1	
$\text{NO}_2^-$	Aqueous + adsorbed Fe(II) (Nontronite)	Abiotic	-2.3	-4.5	0.5	(Grabb et al., 2017)
$\text{NO}_2^-$	Green rust	Abiotic	-4.2 to -9.4	-4.1 to -9.4	0.8 to 1.1	
$\text{NO}_2^-$	Aqueous $\text{Fe}^{2+}$	Abiotic	-6.1 to -33.9	-5.7 to -24.8	0.8 to 1.6	
$\text{NO}_2^-$	Aqueous + adsorbed Fe(II) (Goethite)	Abiotic	-5.9 to -44.8	-5.2 to -33.0	1.0 to 1.4	(Buchwald et al., 2016)
$\text{NO}_2^-$	Aqueous $\text{Fe}^{2+}$	Abiotic	-12.9	-9.8	1.3	(Jones et al., 2015)



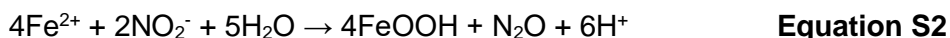
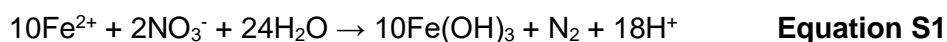
## **Section S1. Micro-sized minerals preparation and magnetite size reduction**

Magnetite (Mag) was obtained from “Mina Cala” (Huelva, Spain), siderite (Sd) from “El guarnón” (Güéjar Sierra, Granada, Spain) and olivine (Ol) from Canet d’Adri (Girona, Spain). The minerals were milled in a vibratory disc mill (RETSCH, RS 100) using a tungsten carbide bowl (WC 94%, Co 6%) and sieved to obtain the fraction with a particle size below 30  $\mu\text{m}$ . An aliquot of Mag microparticles was then milled in a planetary ball mill (FRITSCH, PULVERISETTE P5) at 200 rpm during 15 h, using a stainless steel bowl, deionized water and 0.4 mm steel balls (S110) as grinding media to obtain nanoparticles.

## Section S2. Mineral characterization

The main composition of the minerals was estimated by X-Ray Diffraction (XRD, PANalytical X'Pert PRO), the particle size of the Mag micro and nanoparticles was determined by Laser Diffraction Particle Size Analysis (LDPSA, LS13320, BeckmanCoulter) and morphology by Field Emission Scanning Electron Microscopy (FESEM, JSM-7610F, JEOL).

XRD analysis showed a purity of around 90% for Mag (Fe(II)Fe(III)<sub>2</sub>O<sub>4</sub>), 30% for Sd (Fe(II)CO<sub>3</sub>) and 80% for Ol (Forsterite ferroan, Fe(II)<sub>0.2</sub>Mg<sub>1.8</sub>SiO<sub>4</sub>). Therefore, the given Fe(II)/N molar ratio of the minerals in the microbial experiments was approximately 24 for Mag and Mag-NP, 13 for Sd and 7 for Ol. For Mag calculations, the Fe(II)/Fe(III) ratio was considered stoichiometric although it was not analyzed. In the abiotic experiments (AbFeNO<sub>3</sub> and AbFeNO<sub>2</sub>), the ratio was reduced by half, but dissolved Fe<sup>2+</sup> was added at a Fe<sup>2+</sup>/N of 5. Therefore, although using the same quantity of mineral, in the experiments containing Mag and Mag-NP, the Fe(II) availability could be higher compared to Sd, and the Ol experiments could present the lowest electron donor availability. The stoichiometric Fe(II)/N reported for the NO<sub>3</sub><sup>-</sup> and NO<sub>2</sub><sup>-</sup> reductions are 5 and 2, respectively (**Equation S1** and **S2**) (Melton et al., 2014; Tai and Dempsey, 2009).



According to the LDPSA analysis, the first milling and sieving step gave solid particles with an average Mag particle diameter of 8.12 μm (between 0.07 and 36.24 μm) and the second milling step gave aggregates with an average of 1.16 μm (between 0.04 and 2.00 μm) (Supplementary information, **Figure S1A**). The % volume mode was used for calculations. Although the particle diameter range was wide, a 10 fold decrease in the

mineral size was observed in the Mag-NP compared to the micro-sized Mag. Such decrease was confirmed by the FESEM images, where it was observed that Mag-NP aggregates are formed by smaller nanoparticles with an average particle diameter around 100 nm (Supplementary information, **Figure S1B**).

## REFERENCES

- Melton, E.D., Swanner, E.D., Behrens, S., Schmidt, C., Kappler, A., 2014. The interplay of microbially mediated and abiotic reactions in the biogeochemical Fe cycle. *Nat. Rev. Microbiol.* 12, 797–808. <https://doi.org/10.1038/nrmicro3347>
- Tai, Y.L., Dempsey, B.A., 2009. Nitrite reduction with hydrous ferric oxide and Fe(II): Stoichiometry, rate, and mechanism. *Water Res.* 43, 546–552. <https://doi.org/10.1016/j.watres.2008.10.055>



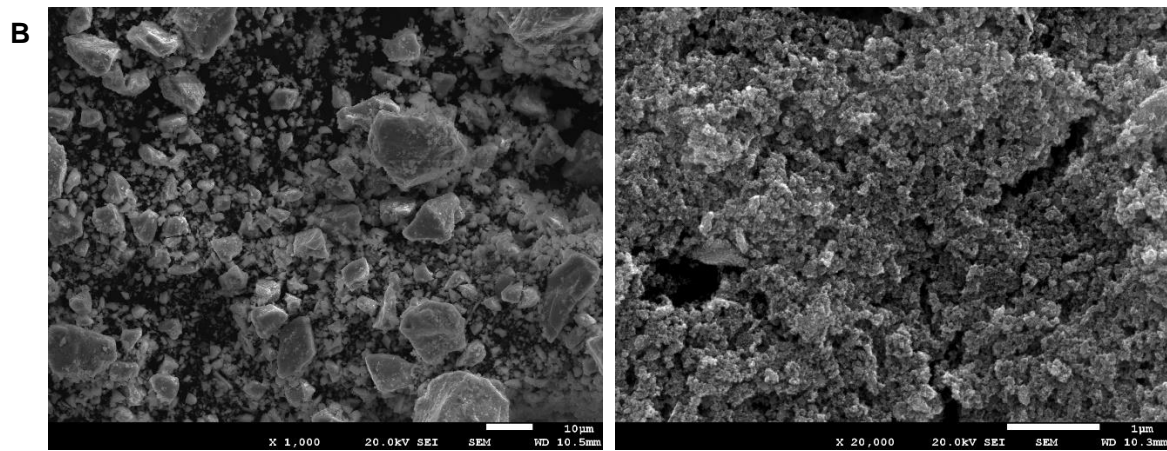
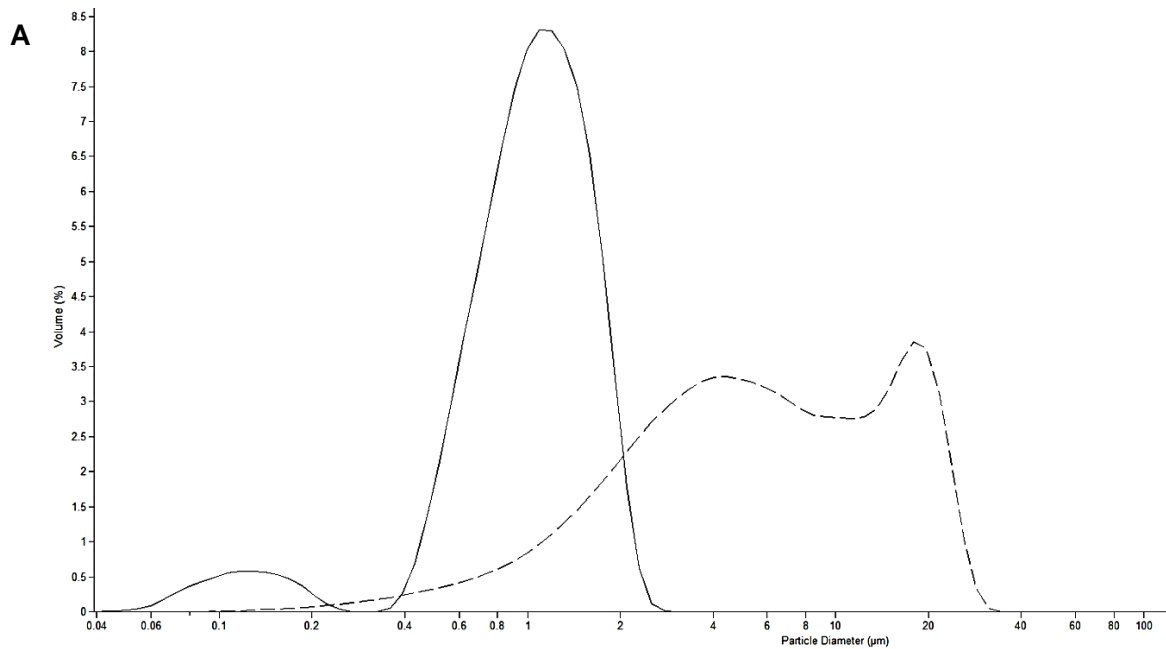


**Figure S1. Mag particles characterization.** **A.** Particle diameter before (dashed line) and after (continuous line) the second milling step. **B.** Particle morphology before (left) and after (right) the second milling step.

**Table S1. Water composition for each series of experiments.** Groundwater was used in the BioSedGW experiments, deionized water (DIW) in the BioSedDIW experiments and synthetic water (produced with DIW) in the AbFeNO<sub>3</sub>, AbFeNO<sub>2</sub> and AbNO<sub>2</sub> experiments (see **Table 1**). Concentrations are expressed in ppm.

	BioSedGW	BioSedDIW	AbFeNO <sub>3</sub>	AbFeNO <sub>2</sub> and AbNO <sub>2</sub>
NaHCO <sub>3</sub>	-	-	306.9	347.6
KH <sub>2</sub> PO <sub>4</sub>	-	-	4.9	7.0
MgCl <sub>2</sub> ·6H <sub>2</sub> O	-	-	259.9	275.6
KCl	-	-	107.3	116.0
CaCl <sub>2</sub> ·2H <sub>2</sub> O	-	-	124.8	99.3
Na <sub>2</sub> SO <sub>4</sub>	-	-	210.0	219.5
KNO <sub>2</sub>	-	-	-	124.8
NaNO <sub>3</sub>	-	97.7	0.104	-
Groundwater NO <sub>3</sub> <sup>-</sup>	71.3	-	-	-
Groundwater NPDOC	2.26	-	-	-

**Table S2.1. Results for de BioSedGW experiments.** Chemical and isotopic characterization. n.d. = non determined.

	Days	pH	NO <sub>3</sub> <sup>-</sup> (mM)	NO <sub>2</sub> <sup>-</sup> (mM)	NH <sub>4</sub> <sup>+</sup> (mM)	N <sub>2</sub> O (nmol)	δ <sup>15</sup> N-NO <sub>3</sub> <sup>-</sup> (‰)	δ <sup>18</sup> O-NO <sub>3</sub> <sup>-</sup> (‰)	δ <sup>15</sup> N-N <sub>2</sub> O (‰)	δ <sup>18</sup> O-N <sub>2</sub> O (‰)
Groundwater	0	7.6	1.15	0.00	n.d.	n.d.	+11.3	+10.1	n.d.	n.d.
BioSedGW-Mag-NP-1	7	5.8	0.80	0.05	0.00	7.1	+15.3	+14.3	-2.6	-41.2
BioSedGW-Mag-NP-2	34	n.d.	0.72	0.00	0.00	12.6	+24.8	+17.9	+20.4	-36.0
BioSedGW-Mag-NP-3	62	7.9	0.20	0.17	n.d.	0.9	+49.4	+44.0	-9.6	-37.7
BioSedGW-Mag-NP-4	71	7.1	0.30	0.13	n.d.	n.d.	+58.0	+30.2	n.d.	n.d.
BioSedGW-Mag-NP-5	78	7.1	0.21	0.17	0.00	38.2	+64.5	+29.8	-6.8	-33.9
BioSedGW-Mag-NP-6	84	7.2	0.17	0.18	n.d.	34.0	+71.0	+27.7	+2.9	-16.1
BioSedGW-Mag-NP-7	91	7.2	0.05	0.19	n.d.	43.3	+90.5	+47.5	+20.6	-26.1
BioSedGW-Mag-NP-8	118	7.1	0.18	0.05	0.00	0.0	+84.0	+20.9	n.d.	n.d.
BioSedGW-Mag-NP-9	222	7.0	0.04	0.00	0.03	63.8	+158.1	+25.0	+64.9	+24.9
BioSedGW-OI-1	7	6.4	0.74	0.07	0.04	0.3	+15.1	+11.8	-29.8	-49.7
BioSedGW-OI-2	62	8.1	0.66	0.16	0.04	0.6	+19.2	+17.1	n.d.	n.d.
BioSedGW-OI-3	84	7.7	0.61	0.01	n.d.	0.6	+15.4	+11.6	-24.2	-32.8

**Table S2.1.** Continued.

	Days	pH	NO <sub>3</sub> <sup>-</sup> (mM)	NO <sub>2</sub> <sup>-</sup> (mM)	NH <sub>4</sub> <sup>+</sup> (mM)	N <sub>2</sub> O (nmol)	δ <sup>15</sup> N-NO <sub>3</sub> <sup>-</sup> (‰)	δ <sup>18</sup> O-NO <sub>3</sub> <sup>-</sup> (‰)	δ <sup>15</sup> N-N <sub>2</sub> O (‰)	δ <sup>18</sup> O-N <sub>2</sub> O (‰)
BioSedGW-OI-4	98	7.6	0.63	0.00	0.02	0.36	n.d.	n.d.	-19.5	-22.0
BioSedGW-OI-5	118	7.6	0.59	0.00	n.d.	0.00	n.d.	n.d.	n.d.	n.d.
BioSedGW-OI-6	222	7.6	0.71	0.00	0.01	0.38	+19.9	+10.1	-1.2	+14.7
BioSedGW-OI-7	365	n.d.	0.74	0.01	0.01	n.d.	n.d.	n.d.	n.d.	n.d.
BioSedGW-Sd-1	7	6.3	0.67	0.17	0.03	3.19	n.d.	n.d.	-4.9	-38.3
BioSedGW-Sd-2	62	7.6	0.43	0.18	0.04	7.43	+21.4	+20.2	-5.7	-46.0
BioSedGW-Sd-3	84	7.1	0.57	0.06	n.d.	11.06	+23.6	+15.8	-3.6	-38.0
BioSedGW-Sd-4	98	7.1	0.52	0.08	n.d.	14.19	n.d.	n.d.	+0.2	-39.0
BioSedGW-Sd-5	118	7.1	0.61	0.00	n.d.	0.00	n.d.	n.d.	n.d.	n.d.
BioSedGW-Sd-6	222	7.0	0.72	0.00	n.d.	6.55	+18.5	+10.1	+6.6	-13.5
BioSedGW-Sd-7	365	n.d.	0.69	0.02	0.01	n.d.	n.d.	n.d.	n.d.	n.d.
BioSedGW-Mag-1	7	6.3	0.69	0.08	0.04	2.42	n.d.	n.d.	-5.9	-36.5
BioSedGW-Mag-2	62	7.6	0.53	0.08	0.01	n.d.	+20.5	+17.1	n.d.	n.d.

**Table S2.1.** Continued.

	Days	pH	NO <sub>3</sub> <sup>-</sup> (mM)	NO <sub>2</sub> <sup>-</sup> (mM)	NH <sub>4</sub> <sup>+</sup> (mM)	N <sub>2</sub> O (nmol)	δ <sup>15</sup> N-NO <sub>3</sub> <sup>-</sup> (‰)	δ <sup>18</sup> O-NO <sub>3</sub> <sup>-</sup> (‰)	δ <sup>15</sup> N-N <sub>2</sub> O (‰)	δ <sup>18</sup> O-N <sub>2</sub> O (‰)
BioSedGW-Mag-3	84	7.2	0.55	0.00	n.d.	35.51	+24.4	+17.0	-2.3	-46.0
BioSedGW-Mag-4	98	7.2	0.53	0.00	0.00	0.94	n.d.	n.d.	-8.5	-17.4
BioSedGW-Mag-5	118	7.2	0.58	0.00	n.d.	3.16	n.d.	n.d.	-3.8	-38.3
BioSedGW-Mag-6	222	7.0	0.57	0.00	0.01	11.88	+24.4	+13.3	-11.3	-28.6
BioSedGW-Mag-7	365	n.d.	0.62	0.02	0.01	n.d.	n.d.	n.d.	n.d.	n.d.
BioSedGW-C-1	7	6.1	0.63	0.08	n.d.	6.87	+15.3	+13.7	-4.0	-42.0
BioSedGW-C-2	84	7.1	0.64	0.00	n.d.	0.00	n.d.	n.d.	n.d.	n.d.
BioSedGW-C-3	222	6.9	0.53	0.06	n.d.	n.d.	+29.2	+20.9	n.d.	n.d.

**Table S2.2. ICP results for de BioSedGW-Mag-NP experiments.** The results are expressed in ppm (semiquantitative). Pb, Cd, Co, Cu, Zn, Al, Be, Li, Mo, Ni, Sb, Ti, Tl, V, As, Cr, P, Se were also analyzed but concentrations were below detection limit. <d.l. = below detection limit. These results are not reported in the manuscript.

	Groundwater	BioSedGW- Mag-NP-1	BioSedGW- Mag-NP-2	BioSedGW- Mag-NP-4	BioSedGW- Mag-NP-5	BioSedGW- Mag-NP-6	BioSedGW- Mag-NP-7	BioSedGW- Mag-NP-8
Ca	92.73	113.63	116.47	98.91	108.03	102.82	100.53	96.00
Na	28.07	31.17	31.47	29.68	31.40	30.77	30.50	29.94
Mg	25.86	28.10	28.90	24.96	26.71	26.13	25.71	25.27
S	23.93	27.81	28.15	25.87	29.00	27.71	27.09	26.16
Si	13.70	5.56	4.64	4.70	4.59	4.54	4.67	4.15
K	5.04	5.80	4.91	4.84	10.21	12.61	5.88	6.02
B	2.85	2.72	2.75	2.97	2.86	3.36	3.13	2.97
Sr	1.13	0.72	0.67	0.64	0.66	0.64	0.63	0.60
Ba	0.05	< d.l.	<d.l.	0.01	<d.l.	<d.l.	0.01	<d.l.
Fe	0.02	0.04	0.03	0.02	0.02	0.03	0.03	0.01
Mn	0.00	0.15	0.15	0.06	0.07	0.07	0.06	0.06

**Table S2.3. Results for de BioSedDIW experiments.** Chemical and isotopic characterization. n.d. = non determined.

	Days	pH	NO <sub>3</sub> <sup>-</sup> (mM)	NO <sub>2</sub> <sup>-</sup> (mM)	NH <sub>4</sub> <sup>+</sup> (mM)	N <sub>2</sub> O (nmol)	δ <sup>15</sup> N-NO <sub>3</sub> <sup>-</sup> (‰)	δ <sup>18</sup> O-NO <sub>3</sub> <sup>-</sup> (‰)	δ <sup>15</sup> N-N <sub>2</sub> O (‰)	δ <sup>18</sup> O-N <sub>2</sub> O (‰)
DIW	0	n.d.	1.15	0.00	n.d.	n.d.	+16.9	+28.5	n.d.	n.d.
BioSedDIW-OI-1	7	6.4	0.65	0.37	n.d.	0.12	+28.7	+43.9	-36.1	-48.3
BioSedDIW-OI-2	91	8.9	0.61	0.38	n.d.	0.18	n.d.	n.d.	-15.7	-40.8
BioSedDIW-OI-3	222	8.6	0.60	0.57	n.d.	n.d.	n.d.	n.d.	n.d.	n.d.
BioSedDIW-Sd-1	7	6.3	0.63	0.50	n.d.	0.24	n.d.	n.d.	-18.8	-44.2
BioSedDIW-Sd-2	91	7.8	0.38	0.47	n.d.	0.14	+24.2	+49.2	-12.8	-45.2
BioSedDIW-Sd-3	222	7.5	0.44	0.73	n.d.	n.d.	n.d.	n.d.	n.d.	n.d.
BioSedDIW-Mag-1	7	5.6	0.42	0.63	n.d.	0.11	n.d.	n.d.	-29.8	-46.3
BioSedDIW-Mag-2	91	8.1	0.52	0.29	n.d.	0.11	n.d.	n.d.	-18.5	-43.2
BioSedDIW-Mag-3	222	7.8	0.57	0.57	n.d.	n.d.	+15.1	+22.6	n.d.	n.d.
BioSedDIW-Mag-NP-1	7	5.8	0.79	0.32	n.d.	0.21	+20.5	+35.9	-28.5	-45.2
BioSedDIW-Mag-NP-2	91	7.8	0.46	0.19	n.d.	0.24	+29.8	+39.2	-10.3	-61.0
BioSedDIW-Mag-NP-3	222	7.6	0.44	0.28	n.d.	n.d.	n.d.	n.d.	n.d.	n.d.

**Table S2.3.** Continued.

	Days	pH	NO <sub>3</sub> <sup>-</sup> (mM)	NO <sub>2</sub> <sup>-</sup> (mM)	NH <sub>4</sub> <sup>+</sup> (mM)	N <sub>2</sub> O (nmol)	δ <sup>15</sup> N-NO <sub>3</sub> <sup>-</sup> (‰)	δ <sup>18</sup> O-NO <sub>3</sub> <sup>-</sup> (‰)	δ <sup>15</sup> N-N <sub>2</sub> O (‰)	δ <sup>18</sup> O-N <sub>2</sub> O (‰)
BioSedDIW-C-1	91	8.2	0.73	0.08	n.d.	0.00	n.d.	n.d.	n.d.	n.d.
BioSedDIW-C-2	222	n.d.	1.10	0.02	n.d.	n.d.	+16.34	+20.1	n.d.	n.d.



**Table S2.4. Results for de AbFeNO3 experiments.** Chemical and isotopic characterization. n.d. = non determined.

	Days	pH	NO <sub>3</sub> <sup>-</sup> (mM)	NO <sub>2</sub> <sup>-</sup> (mM)	N <sub>2</sub> O (nmol)	δ <sup>15</sup> N-NO <sub>3</sub> <sup>-</sup> (‰)	δ <sup>18</sup> O-NO <sub>3</sub> <sup>-</sup> (‰)
Synthetic water	0	n.d.	1.48	0.00	n.d.	+16.9	+28.5
AbFeNO3-Mag-1	50	4.1	n.d.	n.d.	0.00	n.d.	n.d.
AbFeNO3-Mag-2	222	n.d.	1.04	0.02	n.d.	n.d.	n.d.
AbFeNO3-OI-1	50	4.4	n.d.	n.d.	0.00	n.d.	n.d.
AbFeNO3-OI-2	222	n.d.	1.12	0.01	n.d.	n.d.	n.d.
AbFeNO3-Sd-1	50	4	n.d.	n.d.	0.00	+16.7	+28.6
AbFeNO3-Sd-2	222	n.d.	1.28	0.01	n.d.	n.d.	n.d.
AbFeNO3-C-1	50	6.4	n.d.	n.d.	0.00	n.d.	n.d.
AbFeNO3-C-2	222	n.d.	1.26	0.01	n.d.	n.d.	n.d.

**Table S2.5. Results for de AbNO2 experiments.** Chemical characterization.

	Days	NO <sub>3</sub> <sup>-</sup> (mM)	NO <sub>2</sub> <sup>-</sup> (mM)
Synthetic water	0	0.00	1.52
AbNO2-Mag-1	222	0.01	1.26
AbNO2-Mag-2	365	0.01	1.38
AbNO2-OI-1	222	0.00	1.13
AbNO2-OI-2	365	0.02	1.23
AbNO2-Sd-1	222	0.01	1.24
AbNO2-Sd-2	365	0.11	1.11

**Table S2.6. Results for de AbFeNO2 experiments.** Chemical and isotopic characterization. n.d. = non determined.

	Hours	NO <sub>2</sub> <sup>-</sup> (mM)	NH <sub>4</sub> <sup>+</sup> (mM)	N-N <sub>2</sub> O (μmol)	Fe (mM)	δ <sup>15</sup> N-NO <sub>2</sub> <sup>-</sup> (‰)	δ <sup>18</sup> O-NO <sub>2</sub> <sup>-</sup> (‰)
Synthetic water	0	1.10	n.d.	n.d.	5.00	-28.5	n.d.
AbFeNO2-Sd-1	2	1.06	0.0	n.d.	3.30	-27.4	-51.8
AbFeNO2-Sd-2	8	0.87	0.0	n.d.	2.81	-24.1	-49.2
AbFeNO2-Sd-3	23	0.41	0.0	n.d.	1.58	-14.5	-40.6
AbFeNO2-Sd-4	32	0.08	0.0	n.d.	1.60	n.d.	n.d.
AbFeNO2-Sd-5	47	0.07	0.0	n.d.	1.56	n.d.	n.d.
Synthetic water	0	1.54	n.d.	n.d.	5.00	-28.5	n.d.
AbFeNO2-Mag-1	4	1.59	n.d.	0.0	n.d.	-28.8	-46.9
AbFeNO2-Mag-2	8	1.57	n.d.	0.1	n.d.	-28.1	-49.5
AbFeNO2-Mag-3	22	1.42	n.d.	0.7	n.d.	-26.8	-48.1
AbFeNO2-Mag-4	30	1.04	n.d.	2.1	3.26	-24.2	-49.1
AbFeNO2-Mag-5	46	0.92	n.d.	6.2	n.d.	-20.1	-45.6
AbFeNO2-Mag-6	78	0.92	n.d.	n.d.	n.d.	-22.5	n.d.

**Table S2.6.** Continued.

	Hours	NO <sub>2</sub> <sup>-</sup> (mM)	NH <sub>4</sub> <sup>+</sup> (mM)	N-N <sub>2</sub> O (μmol)	Fe (mM)	δ <sup>15</sup> N-NO <sub>2</sub> <sup>-</sup> (‰)	δ <sup>18</sup> O-NO <sub>2</sub> <sup>-</sup> (‰)
AbFeNO2-Mag-7	94	0.90	n.d.	5.1	2.38	-22.6	-43.4
AbFeNO2-Mag-8	114	0.75	n.d.	6.5	2.62	-14.9	-41.9
AbFeNO2-OI-1	4	1.43	n.d.	0.6	n.d.	-27.7	-39.9
AbFeNO2-OI-2	8	1.37	n.d.	1.0	n.d.	-28.8	-38.5
AbFeNO2-OI-3	22	1.32	n.d.	3.3	n.d.	-25.8	-38.1
AbFeNO2-OI-4	30	0.91	n.d.	4.7	2.80	-21.4	-43.7
AbFeNO2-OI-5	46	0.86	n.d.	7.1	n.d.	-19.7	-42.7
AbFeNO2-OI-6	78	0.72	n.d.	n.d.	n.d.	-17.6	-42.4
AbFeNO2-OI-7	114	0.45	n.d.	9.0	2.20	-12.2	-38.9
AbFeNO2-OI-8	168	0.22	n.d.	n.d.	3.23	7.1	n.d.

**Table S2.6.** Continued.

	Hours	NO <sub>2</sub> <sup>-</sup> (mM)	NH <sub>4</sub> <sup>+</sup> (mM)	N-N <sub>2</sub> O (μmol)	Fe (mM)	δ <sup>15</sup> N-NO <sub>2</sub> <sup>-</sup> (‰)	δ <sup>18</sup> O-NO <sub>2</sub> <sup>-</sup> (‰)
AbFeNO2-C-1	4	1.52	n.d.	0.1	n.d.	-29.0	-44.6
AbFeNO2-C-2	8	1.53	n.d.	0.1	n.d.	-28.5	-42.3
AbFeNO2-C-3	22	1.49	n.d.	0.6	n.d.	-26.8	-43.6
AbFeNO2-C-4	30	1.10	n.d.	2.3	3.77	-24.5	-47.8
AbFeNO2-C-5	46	0.86	n.d.	5.8	n.d.	-21.3	-44.4
AbFeNO2-C-6	78	0.97	n.d.	n.d.	n.d.	-22.9	n.d.
AbFeNO2-C-7	114	0.78	n.d.	6.1	2.89	-16.8	-42.4
AbFeNO2-C-8	168	0.00	n.d.	n.d.	2.96	n.d.	n.d.

**Table S2.7. ICP results for de AbFeNO2 experiments.** The results are expressed in ppm (semiquantitative). Pb, Al, Be, Li, Mo, Sb, Ti, Tl, V, As, Cr and Se were also analyzed but concentrations were below detection limit. <d.l. = below detection limit; h = hours. The employed instrument for the analysis was: Perkin Elmer Optima 8300. These results are not reported in the manuscript.

	h	Ca	Mg	Ba	Cd	Co	Cu	Mn	Sr	Zn	K	Ni	Na	B	P	S	Si
AS	0	23.41	30.99	0.01	<d.l.	<d.l.	<d.l.	<d.l.	0.01	0.03	117.29	<d.l.	165.38	<d.l.	2.12	45.58	<d.l.
AbFeNO2-Sd-1	2	38.05	30.71	0.11	<d.l.	0.03	0.06	10.93	0.06	0.06	95.81	<d.l.	150.06	0.20	<d.l.	45.04	0.65
AbFeNO2-Sd-2	8	37.74	32.19	0.14	<d.l.	0.04	0.05	14.94	0.07	0.05	94.13	<d.l.	146.97	<d.l.	<d.l.	42.72	0.53
AbFeNO2-Sd-3	23	38.77	32.33	0.17	<d.l.	0.04	0.06	22.07	0.08	0.06	93.14	<d.l.	148.32	1.12	<d.l.	37.70	1.43
AbFeNO2-Sd-4	32	41.00	34.17	0.18	0.01	0.05	0.08	24.32	0.09	0.08	93.98	<d.l.	149.81	0.97	<d.l.	38.41	1.30
AbFeNO2-Sd-5	47	39.89	32.74	0.18	<d.l.	0.05	0.08	25.42	0.09	0.09	92.96	<d.l.	152.08	1.96	<d.l.	38.41	1.70
AbFeNO2-Mag-4	30	23.85	32.97	0.04	0.02	0.03	<d.l.	0.24	0.02	0.07	114.72	<d.l.	161.23	<d.l.	<d.l.	44.17	2.17
AbFeNO2-Mag-5	31	24.05	33.55	0.03	0.01	0.03	<d.l.	0.25	0.02	0.04	118.40	<d.l.	165.56	1.06	<d.l.	44.39	2.38
AbFeNO2-Mag-7	94	26.74	34.82	0.04	0.01	0.03	<d.l.	0.42	0.02	0.09	118.26	<d.l.	164.49	1.95	<d.l.	44.74	3.88
AbFeNO2-Mag-8	114	27.17	35.50	0.04	0.01	0.03	<d.l.	0.43	0.02	0.08	119.65	<d.l.	166.33	<d.l.	<d.l.	45.91	2.83
AbFeNO2-OI-4	30	22.11	46.48	0.02	0.01	0.13	<d.l.	0.12	0.02	0.06	116.82	0.11	165.71	1.06	<d.l.	44.72	4.52
AbFeNO2-OI-5	31	22.03	54.82	0.04	0.04	0.16	<d.l.	0.23	0.02	0.31	115.66	0.24	167.97	2.67	<d.l.	42.75	10.64
AbFeNO2-OI-6	94	21.94	50.31	0.03	0.01	0.15	<d.l.	0.13	0.02	0.04	116.04	0.11	157.48	<d.l.	<d.l.	43.74	5.57
AbFeNO2-OI-7	114	22.55	50.24	0.02	0.01	0.17	<d.l.	0.13	0.02	0.07	118.44	0.16	169.17	2.06	<d.l.	44.82	7.42
AbFeNO2-OI-8	168	24.34	45.69	0.03	0.01	0.11	<d.l.	0.12	0.02	0.09	120.15	0.13	168.44	<d.l.	<d.l.	45.92	5.22

**Table S2.7.** Continued.

	h	Ca	Mg	Ba	Cd	Co	Cu	Mn	Sr	Zn	K	Ni	Na	B	P	S	Si
AbFeNO2-C-4	30	22.37	30.62	0.02	0.02	<d.l.	<d.l.	0.07	0.01	0.06	120.47	<d.l.	162.92	<d.l.	<d.l.	45.14	<d.l.
AbFeNO2-C-5	31	21.76	30.92	0.02	0.01	<d.l.	<d.l.	0.06	0.01	0.03	118.66	<d.l.	166.36	1.38	<d.l.	44.71	1.38
AbFeNO2-C-6	94	21.43	30.22	0.02	0.01	<d.l.	<d.l.	0.06	0.01	0.11	116.97	<d.l.	165.70	2.72	<d.l.	45.04	2.54
AbFeNO2-C-7	114	22.31	31.08	0.02	0.02	<d.l.	<d.l.	0.07	0.01	0.13	118.32	<d.l.	166.67	<d.l.	<d.l.	45.93	<d.l.
AbFeNO2-C-8	168	21.58	30.44	0.04	0.03	<d.l.	<d.l.	0.13	0.01	0.69	117.26	<d.l.	167.29	3.49	<d.l.	35.52	2.06

**Table S2.8. Results of qualitative tests performed previously to the beginning of the present study.** These batch experiments contained synthetic water with NO<sub>3</sub><sup>-</sup> and micro-sized magnetite (bottles 1 to 4 contained 0.3 g, while bottles 5 to 8 contained 1.4 g). Set-up and incubation followed the same conditions than the abiotic experiments reported in **Table 1**. The qualitative concentration results were obtained by nitrate/nitrite test strips (Quantofix, Macherey-Nagel). In the table, for each bottle, the left column show nitrate and the right column nitrite concentrations (mg/L). Shaded cells reflect uncertainty in measurement.

Day/bottle	1		2		3		4		5		6		7		8	
0	100	0	100	0	100	0	100	0	100	0	100	0	100	0	100	0
6	100	0	100	0	100	0	100	0	100	0	100	0	100	0	100	0
14	100	0	100	0	100	0	100	0	100	0	100	0	100	0	100	0
22	100	0.5	100	0	100	0.5	100	0	100	0	100	0	100	0	100	0.5
32	100	0.5	100	0	100	0.5	100	0	100	0	100	0	100	0	100	0.5
42	100	0.5	100	0.5	100	0.5	100	0	100	0.5	100	0.5	100	0	100	0.5
49	100	0	100	0.5	100	0.5	100	0.5	100	0.5	100	0.5	100	0.5	100	0.5
56	100	0	100	0.5	100	0.5	100	0.5	100	0.5	100	0	100	0.5	100	0.5
63	100	0	75	0	100	0.5	100	0.5	-	-	100	0	100	0.5	100	0.5
69	-	-	75	0	100	0.5	100	0.5	-	-	100	0	100	0.5	100	0.5
76	-	-	75	0	100	0.5	100	0.5	-	-	100	0	100	0	100	0.5
86	-	-	100	0	100	0.5	100	0.5	-	-	100	0	100	0	100	0.5
104	-	-	100	0	100	0.5	100	0.5	-	-	100	0	100	0	100	0.5